Chapter 3

Kinematic Analysis

At first glance it may seem surprising how rich and deep the study of mechanism kinematics has become considering how commonplace four-bar linkages are. A mechanical system typically comprises a power source and a linkage that transforms the power into a desired motion in a controlled, predictable, and repeatable way. Our focus will be on the linkage itself, and how to design and analyse the resulting motion. The motion design employs the many techniques of kinematic synthesis, while the study of the generated motion requires the tools and techniques of kinematic analysis, some of which will be examined in this chapter.

Modern day kinematic analysis and synthesis are rooted in the geometry of antiquity: in both the axiomatic structure of synthetic geometry and the metric structure of analytic geometry. Indeed, the modern understanding of axiomatic and non-Euclidean geometries arose from careful reflection on Euclid's work [1] over the course of the last 2400 years. Consider the following quote from [2], page 11:

> The Greeks called an axiomatic approach *synthetic* because it synthesizes `[sic]` (proves) new results from statements already known. The Greeks often used a process they called *analysis* to find new results that they then proved. They analyzed `[sic]` a problem by assuming the desired solution and worked backward to something known. We mimic this procedure in what we call analytic geometry and algebra by assuming that there is an answer, the unknown x, and solving for it. In modern times synthetic geometry has come to mean geometry without coordinates because coordinates are central to analytic geometry.

3.1 Planar Mechanisms

In this section we will examine the elementary kinematics of planar four-bar mechanisms from an advanced standpoint. The last sentence, while true, is a grammatical nod to Felix Klein [3]. Kinematic constraints will first be discussed, followed by a novel development of the input-output (I-O) equation for planar $4R$ mechanisms, which turns out to represent the I-O equation for any planar four-bar topology.

3.1.1 Kinematic Constraints

In the context of mechanism kinematics, a *dyad* is a binary link coupled to two other rigid bodies with two kinematic pairs [4]. In a planar four-bar linkage the two other rigid bodies are a relatively non-moving ground link, while the other is the coupler when coupled to another dyad. For planar displacements there are only two types of lower pair that can be used to generate a planar motion: R- and P-pairs. This means there are only four practical planar dyads

$$RR,\ PR,\ RP, \text{ and } PP.$$

These 3-link serially connected open kinematic chains of rigid bodies are the building blocks of every planar mechanism. They are designated according to the type of joints connecting the rigid links, and listed in series starting with the joint connected to ground, each illustrated in Figure 3.1.

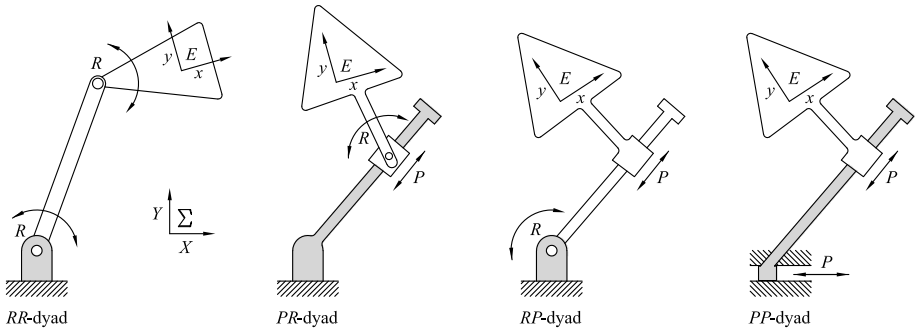

Figure 3.1: Types of dyads.

When a pair of dyads are joined, a four-bar linkage is obtained. However, the designation of the *output* dyad changes. For example, consider a planar four-bar linkage composed of an RR-dyad on the *left-hand side* of the mechanism, and

a PR-dyad on the *right-hand side*, where the *input* link is the *grounded* link in the RR-dyad, see Figure 3.2.

Suppose revolute joint R_1 is actuated by some form of torque supplied by an electric rotary motor transferred by a transmission, in turn driving the input link, l_1. The linkage is designated by listing the joints in sequence from the ground fixed actuated joint, starting with the input link listing the joints in order. Thus, the mechanism composed of a driving RR-dyad, and an output PR-dyad is called an $RRRP$ linkage, where the order of PR is switched to RP. If the output were an RP-dyad, the mechanism would be an $RRPR$ linkage. If the input were an RP-dyad while the output was an RR-dyad, the resulting mechanism would be an $RPRR$ linkage, with no noticeable alteration in the designation.

Since there are only two linearly independent translations and a single rotation available for the displacement of a rigid body in the plane, the maximum number of relative degrees of freedom (DOF) is three. Many mechanical systems are designed to provide only a single DOF meaning that only one motor is needed. Regardless, a planar four-bar linkage can be designed to generate coupled translations and rotations, as in the rigid body guidance problem. In this case the motion of the coupler is considered, link c in Figure 3.3. Alternately, only a fixed axis rotation, or displacement along a fixed line may be the required output. In this case, the linkage is generally termed a *function gener-*

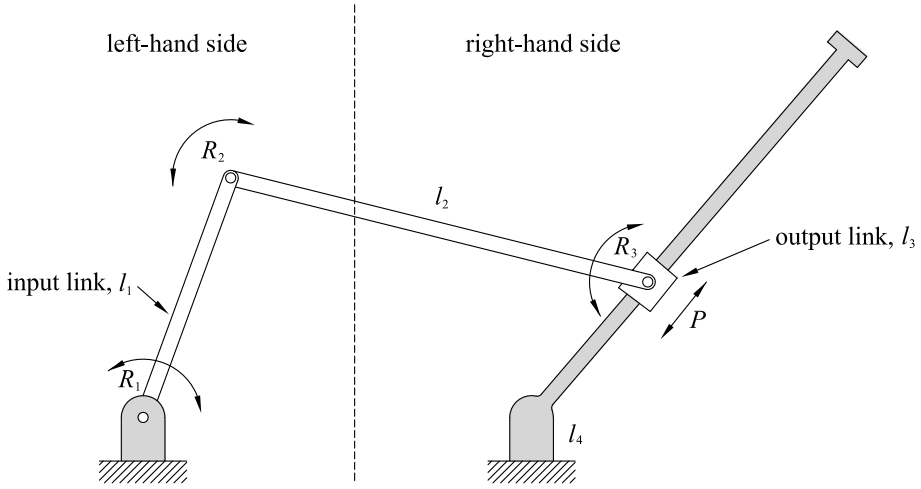

Figure 3.2: A four-bar linkage with RR-dyad on the left-hand side and PR-dyad on the right-hand side.

ator, since it typically uses the linkage geometry to move the output link, link b in Figure 3.3, as a function of the input, link a in this case. The function is generally expressed as the output angle in terms of the input angle, $\varphi = f(\psi)$. The function is inverted if link b is the input while link a is the output.

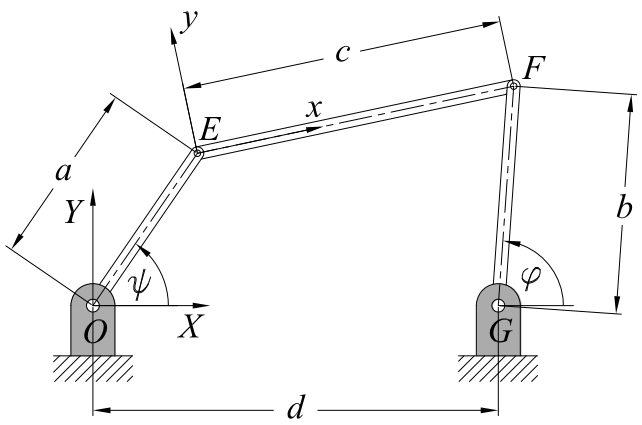

Figure 3.3: 4R four-bar mechanism.

3.1.2 Planar $4R$ Mechanism

The first type of linkage that will be analysed contains four rigid links coupled by four R-pairs forming a simple closed kinematic chain. These linkages are generally denoted as $4R$ mechanisms.

3.1.2.1 Input-output Equation

The material presented in what follows is from [5, 6], but new results are included as well. A planar $4R$ function generator correlates driver and follower angles in a functional relationship. The mechanism essentially generates the function $\varphi = f(\psi)$, or vice versa, see Figure 3.3. Design methods typically employ the Freudenstein synthesis equations to identify link lengths required to generate the function [7, 8]. For over-determined sets of prescribed input-output (I-O) angle pairs, these equations are linear in the three unknown Freudenstein parameters, which are ratios of the link lengths, and can be solved for using any least squares method to minimise a specified performance error. To the best of the authors knowledge, there are no alternative algebraic models of the function generator displacement equations in the accessible literature.

Design and structural errors are important performance indicators in the assessment and optimisation of function generating linkages arising by means of approximate synthesis. The *design error* indicates the error residual incurred by a specific linkage in satisfying its I-O synthesis equations. The *structural error*, in turn, is the difference between the prescribed linkage output value and the actual generated output value for a given input value [9]. From a design point of view it may be successfully argued that the structural error is the one that really matters, for it is directly related to the performance of the linkage.

It has been observed [10, 11] that as the cardinality of the prescribed discrete I-O data set increases, the corresponding four-bar linkages that minimise the Euclidean norm of the design and structural errors tend to converge to the same linkage. The important implication is that minimising the Euclidean norm, or any p-norm, of the structural error can be accomplished indirectly by minimising the same norm of the design error, provided that a suitably large number of I-O pairs is prescribed. The importance arises from the fact that the minimisation of the Euclidean norm of the design error leads to a linear least-squares problem whose solution can be obtained directly as opposed to iteratively [12, 13], while the minimisation of the same norm of the structural error leads to a nonlinear least-squares problem, and hence, calls for an iterative solution [9]. In [11] the trigonometric Freudenstein synthesis equations are integrated in the range between minimum and maximum input values, thereby reposing the discrete approximate synthesis problem as a continuous one whereby the objective function is optimised over the entire I-O range. Hence, the long-term goal of research in this area is to determine a general method to derive motion constraint based algebraic I-O equations that may be used together with the method of continuous approximate synthesis [11] to obtain the very best linkage that can generate an arbitrary function. The goal of what is now presented is to develop one in the hope of providing new insight into the continuous approximate synthesis of function generators, while mitigating numerical integration error. Of course, the same equation will be obtained by making the tangent half-angle substitutions directly into the Freudenstein equation then collecting terms after factoring, normalising, and eliminating non-zero factors. But that must be the case since the geometric relations require that outcome, however this is irrelevant because the goal is to generalise a method to develop constraint based algebraic I-O equations for continuous approximate synthesis of planar, spherical, and spatial linkages.

The Freudenstein equation relating the input to the output angles of a planar $4R$ four-bar mechanism, with link lengths as in Figure 3.3, was first put forward

in [14]. In the equation the angle ψ is traditionally selected to be the input while φ is the output angle:

$$k_1 + k_2\cos(\varphi_i) - k_3\cos(\psi_i) \quad = \quad \cos(\psi_i - \varphi_i). \tag{3.1}$$

Equation (3.1) is linear in the k_i Freudenstein parameters, which are defined in terms of the link length ratios as

$$\left.\begin{array}{rcl} k_1 & \equiv & \dfrac{(a^2+b^2+d^2-c^2)}{2ab}, \\ k_2 & \equiv & \dfrac{d}{a}, \\ k_3 & \equiv & \dfrac{d}{b}. \end{array}\right\} \Leftrightarrow \left\{\begin{array}{rcl} d & = & 1, \\ a & = & \dfrac{1}{k_2}, \\ b & = & \dfrac{1}{k_3}, \\ c & = & (a^2+b^2+d^2-2abk_1)^{1/2}. \end{array}\right.$$

The new idea starts the same as with the Freudenstein method, writing the displacement constraints in terms of the I-O angles. Continuing with tradition, we select ψ to be the input angle and φ to be the output angle, see Figure 3.3. Let Σ be a non moving Cartesian coordinate system with coordinates X and Y whose origin is located at the centre of the ground fixed R-pair connected to the link with length a. Let E be a coordinate system that moves with the coupler of length c whose origin is at the centre of the distal R-pair of link a, having basis directions x and y.

The displacement constraints for the origin of E can be expressed in terms of Σ as

$$\begin{array}{rcl} X - a\cos\psi & = & 0, \\ Y - a\sin\psi & = & 0, \end{array} \tag{3.2}$$

while those for point F, located at the centre of the distal R-pair on the output link with length b are

$$\begin{array}{rcl} X - d - b\cos\varphi & = & 0, \\ Y - b\sin\varphi & = & 0. \end{array} \tag{3.3}$$

Next, we use a planar projection of Study's soma coordinates [15] to establish the I-O equation. While Study's soma will be explained in detail in *Chapter 5: Geometry*, a few words of introduction are given here. Any displacement in Euclidean space, E_3, can be mapped in terms of the coordinates of a 7-

dimensional projective image space using the transformation [16]

$$\mathbf{T} = \begin{bmatrix} x_0^2+x_1^2+x_2^2+x_3^2 & 0 & 0 & 0 \\ 2(-x_0y_1+x_1y_0-x_2y_3+x_3y_2) & x_0^2+x_1^2-x_2^2-x_3^2 & 2(x_1x_2-x_0x_3) & 2(x_1x_3+x_0x_2) \\ 2(-x_0y_2+x_1y_3+x_2y_0-x_3y_1) & 2(x_1x_2+x_0x_3) & x_0^2-x_1^2+x_2^2-x_3^2 & 2(x_2x_3-x_0x_1) \\ 2(-x_0y_3-x_1y_2+x_2y_1+x_3y_0) & 2(x_1x_3-x_0x_2) & 2(x_2x_3+x_0x_1) & x_0^2-x_1^2-x_2^2+x_3^2 \end{bmatrix}. \quad (3.4)$$

This transforms the coordinates of any point described in a moving $3D$ coordinate system E to the coordinates of the same point in a relatively fixed $3D$ coordinate system Σ, assuming that the two coordinate systems are initially coincident, after a given displacement of E relative to Σ in terms of the coordinates of a point on the Study quadric, S_6^2. Study's soma coordinates are the eight ratios

$$(c_0 : c_1 : c_2 : c_3 : g_0 : g_1 : g_2 : g_3).$$

The first four of Study's soma coordinates are the Euler-Rodrigues parameters c_i, which are also the elements of a quaternion [16]. They are defined as

$$\begin{aligned} c_0 &= \cos\tfrac{\varphi}{2}, \\ c_1 &= s_x \sin\tfrac{\varphi}{2}, \\ c_2 &= s_y \sin\tfrac{\varphi}{2}, \\ c_3 &= s_z \sin\tfrac{\varphi}{2}. \end{aligned}$$

When the c_i are normalised such that they represent a unit vector in which case $\mathbf{s} = [s_x, s_y, s_z]^T$ is a unit direction vector parallel to the axis and φ is the angular measure of a given rotation.

The last four g_i linear combinations of the Euler-Rodrigues parameters and elements of the vector elements of the position vector $\mathbf{d} = (d_0 : d_1 : d_2 : d_3)^T$ of the origin of E expressed in Σ. The g_i are defined as

$$\begin{aligned} g_0 &= d_1c_1 + d_2c_2 + d_3c_3, \\ g_1 &= -d_1c_0 + d_3c_2 - d_2c_3, \\ g_2 &= -d_2c_0 - d_3c_1 + d_1c_3, \\ g_3 &= -d_3c_0 + d_2c_1 - d_1c_2. \end{aligned} \quad (3.5)$$

The elements of the transformation in Equation (3.4) are the coordinates of Study's kinematic mapping image space, where distinct $3D$ displacements are represented by distinct points, are given by the following equations in terms of the eight Study soma

$$(x_0 : x_1 : x_2 : x_3 : y_0 : y_1 : y_2 : y_3) = \left(c_0 : c_1 : c_2 : c_3 : \frac{g_0}{2} : \frac{g_1}{2} : \frac{g_2}{2} : \frac{g_3}{2}\right).$$

General points in the kinematic mapping image space are described the eight ratios $\{x_i : y_i\}$. In order for a point in the image space to represent a real displacement, and therefore to be located on S_6^2, the non-zero condition of $x_1^2 + x_2^2 + x_3^2 + x_4^2 \neq 0$ must be satisfied.

The transformation matrix $\mathbf{T}$ simplifies considerably when we consider displacements that are restricted to a plane. Three degrees of freedom are lost and hence four Study parameters vanish. The displacements may be restricted to any plane. Without loss in generality, we may select one of the principal planes in Σ. Thus, we arbitrarily select the plane $Z = 0$. Since E and Σ are assumed to be initially coincident, this means

$$\begin{bmatrix} W \\ X \\ Y \\ 0 \end{bmatrix} = \mathbf{T} \begin{bmatrix} w \\ x \\ y \\ 0 \end{bmatrix}. \tag{3.6}$$

This planar case requires that $d_3 = 0$ since $Z = z = 0$ because reference frame E can translate in neither the Z nor z directions. It also requires that $s_x = s_y = 0$ and $s_z = 1$: the equivalent rotation axis is parallel to both the Z and z axes. This, in turn, annihilates four soma coordinates because

$$\begin{aligned} x_1 = c_1 = s_x \sin\frac{\varphi}{2} &= 0, \\ x_2 = c_2 = s_y \sin\frac{\varphi}{2} &= 0, \\ 2y_0 = g_0 = d_1c_1 + d_2c_2 + d_3c_3 &= 0, \\ 2y_3 = g_3 = -d_3c_0 + d_2c_1 - d_1c_2 &= 0. \end{aligned}$$

Therefore displacements restricted to the plane $Z = z = 0$ leaves us with only the four soma coordinates

$$(x_0 : x_3 : y_1 : y_2). \tag{3.7}$$

The non-zero condition is now $x_0^2 + x_3^2 \neq 0$, and the fourth row and column of the reduced $\mathbf{T}$ contains only this condition as the last element, with zeros elsewhere, leading to the trivial equation $Z = z = 0$. We can therefore eliminate the fourth row and column and normalise the coordinates with the nonzero condition giving the planar mapping equation

$$\mathbf{T} = \frac{1}{x_0^2 + x_3^2} \begin{bmatrix} x_0^2 + x_3^2 & 0 & 0 \\ 2(-x_0y_1 + x_3y_2) & x_0^2 - x_3^2 & -2x_0x_3 \\ -2(x_0y_2 + x_3y_1) & 2x_0x_3 & x_0^2 - x_3^2 \end{bmatrix}. \tag{3.8}$$

We can now express a point in Σ in terms of the soma coordinates and the corresponding point coordinates in E as

$$\begin{bmatrix} 1 \\ X \\ Y \end{bmatrix} = \mathbf{T} \begin{bmatrix} 1 \\ x \\ y \end{bmatrix} = \frac{1}{x_0^2+x_3^2} \begin{bmatrix} x_0^2+x_3^2 \\ 2(-x_0y_1+x_3y_2)+(x_0^2-x_3^2)x-(2x_0x_3)y \\ -2(x_0y_2+x_3y_1)+(2x_0x_3)x+(x_0^2-x_3^2)y \end{bmatrix}. \tag{3.9}$$

The novelty of the approach begins with the creation of two Cartesian vector constraint equations containing the nonhomogeneous coordinates in Equations (3.2) and (3.3), but substituting the values in Equation (3.9) for (X, Y). These two vector equations are $\mathbf{F}_1 = \mathbf{0}$ and $\mathbf{F}_2 = \mathbf{0}$:

$$\mathbf{F}_1 = \frac{1}{x_0^2+x_3^2} \begin{bmatrix} 2(-x_0y_1+x_3y_2)+(x_0^2-x_3^2)x-2x_0x_3y-(a\cos\psi)(x_0^2+x_3^2) \\ -2(x_0y_2+x_3y_1)+2x_0x_3x+(x_0^2-x_3^2)y-(a\sin\psi)(x_0^2+x_3^2) \end{bmatrix} = \mathbf{0};$$

$$\mathbf{F}_2 = \frac{1}{x_0^2+x_3^2} \begin{bmatrix} 2(-x_0y_1+x_3y_2)+(x_0^2-x_3^2)x-2x_0x_3y-(b\cos\varphi+d)(x_0^2+x_3^2) \\ -2(x_0y_2+x_3y_1)+2x_0x_3x+(x_0^2-x_3^2)y-(b\sin\varphi)(x_0^2+x_3^2) \end{bmatrix} = \mathbf{0}.$$

Now we determine equations for the coupler. The coordinate system that moves with the coupler has its origin, point E, on the centre of the R-pair, as in Figure 3.3, having coordinates $(x, y) = (0, 0)$, while point F is on the R-pair centre on the other end having coordinates $(x, y) = (c, 0)$. One more vector equation, $\mathbf{H}_1$ is obtained by substituting $(x, y) = (0, 0)$ in $\mathbf{F}_1$, and another, $\mathbf{H}_2$ is obtained by substituting $(x, y) = (c, 0)$ in $\mathbf{F}_2$. Next $\mathbf{H}_1$ and $\mathbf{H}_2$, two rational expressions, are converted to factored normal form. This is the form where the numerator and denominator are relatively prime polynomials with integer coefficients. The denominators for both $\mathbf{H}_1$ and $\mathbf{H}_2$ are the nonzero condition $x_0^2 + x_3^2$, which can safely be factored out of each equation leaving the following two vector equations with polynomial elements:

$$\mathbf{H}_1 = \begin{bmatrix} -a\cos\psi(x_0^2+x_3^2)+2(-x_0y_1+x_3y_2) \\ -a\sin\psi(x_0^2+x_3^2)-2(x_0y_1+x_3y_2) \end{bmatrix} = \mathbf{0}; \tag{3.10}$$

$$\mathbf{H}_2 = \begin{bmatrix} -(b\cos\varphi+d)(x_0^2+x_3^2)+c(x_0^2-x_3^2)+2(-x_0y_1+x_3y_2) \\ -b\sin\varphi(x_0^2+x_3^2)+2c(x_0x_3)-2(x_0y_2+x_3y_1) \end{bmatrix} = \mathbf{0}. \tag{3.11}$$

The system of four displacement constraints on the I-O equations are $\mathbf{H}_1 = \mathbf{0}$ and $\mathbf{H}_2 = \mathbf{0}$. However, these are trigonometric equations. We convert them to

algebraic ones using the tangent of the half-angle substitutions

$$u = \tan\frac{\psi}{2}, \quad v = \tan\frac{\varphi}{2},$$

and

$$\begin{aligned} \cos\psi &= \frac{1-u^2}{1+u^2}, \quad \sin\psi = \frac{2u}{1+u^2}, \\ \cos\varphi &= \frac{1-v^2}{1+v^2}, \quad \sin\varphi = \frac{2v}{1+v^2}. \end{aligned}$$

The usual constraint equations in the kinematic mapping image space are obtained by considering $\mathbf{H}_1$ and $\mathbf{H}_2$ with the tangent of the half-angles, giving four new algebraic polynomials when considering the individual elements converted to factored normal form. The denominators are u^2+1 and v^2+1 which can safely be factored out because they are always non-vanishing. The resulting four algebraic equations are expressed in terms of the elements of $\mathbf{K}_1 = \mathbf{0}$ and $\mathbf{K}_2 = \mathbf{0}$:

$$\mathbf{K}_1 = \begin{bmatrix} (au^2-a)(x_0^2+x_3^2)+2u^2(-x_0y_1+x_3y_2)+2(-x_0y_2+x_3y_1) \\ \\ -2au(x_0^2+x_3^2)-2(1+u^2)(-x_0y_2+x_3y_1) \end{bmatrix} = \mathbf{0}; \tag{3.12}$$

$$\mathbf{K}_2 = \begin{bmatrix} (v^2(b-d)+b-d)(x_0^2+x_3^2)+(cv^2+c)(x_0^2-x_3^2)+2(1+v^2)(-x_0y_1+x_3y_2) \\ \\ 2(v^2+1)(cx_0x_3-x_0y_2-x_3y_1)-2bv(x_0^2+x_3^2) \end{bmatrix} = \mathbf{0}. \tag{3.13}$$

Factoring the resultant of the first and second elements of $\mathbf{K}_1 = \mathbf{0}$ with respect to u, as well as the first and second elements of $\mathbf{K}_2 = \mathbf{0}$ with respect to v yields the two displacement constraint equations in the image space:

$$a^2(x_0^2+x_3^2) - 4(y_1^2+y_2^2) = 0,$$

$$\begin{aligned} (\,b^2-c^2-d^2)(x_0^2+x_3^2) + 2cd(x_0^2-x_3^2) + 4c(x_0y_1+x_3y_2) + \\ 4d(-x_0y_1+x_3y_2) - 4(y_1^2+y_2^2) = 0. \end{aligned}$$

Inspection of the quadratic forms of these two equations reveals that they are two hyperboloids of one sheet, which is exactly what is expected for two RR dyads [17]. But these are not the constraints we are looking for. We want to eliminate the image space coordinates using $\mathbf{K}_1 = \mathbf{0}$ and $\mathbf{K}_2 = \mathbf{0}$ to obtain an algebraic polynomial with the tangent half angles u and v as variables and link lengths as coefficients.

To obtain this algebraic polynomial we start by setting the homogenising coordinate $x_0 = 1$, which can safely be done since we are only concerned with

real finite displacements. Next, observe that the two equations represented by the components of $\mathbf{K}_1 = \mathbf{0}$ (Equation (3.12)) have a simpler form than those of $\mathbf{K}_2 = \mathbf{0}$ (Equation (3.13)), and are linear in y_1 and y_2. Solving these two equations for y_1 and y_2 reveals that

$$y_1 = \frac{1}{2}\frac{a(u^2 - 2ux_3 - 1)}{u^2 + 1}, \tag{3.14}$$

$$y_2 = \frac{1}{2}\frac{a(u^2x_3 + 2u - x_3)}{u^2 + 1}. \tag{3.15}$$

Equations (3.14) and (3.15) reveal the common denominator of u^2+1, which can never be less than 1, and hence may be factored out. Now we back-substitute these expressions for y_1 and y_2 into the array components of Equation (3.13), thereby eliminating these image space coordinates, and factor the resultant with respect to x_3 which yields four factors. The first three are

$$4c^2, \;\; (u^2 + 1)^3, \;\; (v^2 + 1)^3.$$

None of these three factors can ever be zero and at the same time represent a real displacement constraint, hence they are eliminated. The remaining factor is a polynomial with only u and v as variables and link lengths a, b, c, and d, as coefficients. This is exactly the constraint equation we desire. It is factored, and the terms collected then distributed over u and v revealing

$$Au^2v^2 + Bu^2 + Cv^2 - 8abuv + D = 0, \tag{3.16}$$

where:

$$\begin{aligned} A &= (a - b - c + d)(a - b + c + d) = A_1A_2; \\ B &= (a + b - c + d)(a + b + c + d) = B_1B_2; \\ C &= (a + b - c - d)(a + b + c - d) = C_1C_2; \\ D &= (a - b + c - d)(a - b - c - d) = D_1D_2. \end{aligned}$$

Equation (3.16) is an algebraic polynomial of degree four which represents the I-O equation for any planar $4R$ mechanism. As shown in [6], it has two singular points at infinity, namely those of the u- and v-axes, see Section 3.6.2.4. Singular points on planar algebraic curves are individual points of the curve, if they exist, that are unique compared to the regular points on the curve in that they not only satisfy the equation of the curve but they also possess special distinct properties. The existance of singular points can be determined by homogenising the equation. We will use the new coordinate w and redefine

the angle parameter values as u/w and v/w, and manipulate the equation by multiplying it through by w to obtain a version of the I-O equation that is homogeneously of degree four in all variables u, v, and w, resulting in the new homogeneous expression of curve k_h:

$$k_h := \quad Au^2v^2 + Bu^2w^2 + Cv^2w^2 - 8abuvw^2 + Dw^4 \quad = \quad 0. \qquad (3.17)$$

The singular values of Equation (3.17), if they exist, are determined by solving the three partial derivatives of k_h with respect to the three variables u, v, and w. These three homogeneous equations of degree three are

$$\left.\begin{array}{rcrcl} \dfrac{\partial k_h}{\partial u} & = & 2Auv^2 + 2Buw^2 - 8abvw^2 & = & 0, \\ \dfrac{\partial k_h}{\partial v} & = & 2Au^2v + 2Cvw^2 - 8abuw^2 & = & 0, \\ \dfrac{\partial k_h}{\partial w} & = & 2Bu^2w + 2Cv^2w - 16abvw + 4Dw^3 & = & 0. \end{array}\right\} \qquad (3.18)$$

Equations (3.18) have two common solutions which are independent of the link lengths a, b, c, and d embedded in the coefficients A, B, C, and D:

$$S_1 := \{u = 1, v = 0, w = 0\}, \quad S_2 := \{u = 0, v = 1, w = 0\}. \qquad (3.19)$$

These two points, called *double points*, common to all algebraic I-O curves for every planar $4R$ four-bar mechanism are the points on the line at infinity $w = 0$ of the u- and v-axes, respectively. Each of these double points can have real or complex tangents depending on the values of the link lengths, which in turn determines the nature of the mobility of the linkage, as well as the number of assembly modes (the maximum is two), and the number of folding assemblies (the maximum is three). Each of these two double points can be either *crunodes* where the curve intersects itself, or acnodes, which are isolated, or hermit points in the solution set of a polynomial equation in two real variables, again see Section 3.6.2.4. When both are crunodes the mechanism is a double crank, when both are acnodes the mechanism is a double rocker. In the event the mechanism is a folding four-bar then the degree of Equation (3.16) is less than four.

It is the nature of the tangents at the double points that determine the mobility of the input and output links. Both double points can have real, or complex tangents, depending on the values of the four link lengths. The possible combinations of these cases have different meanings for the corresponding linkages. The following three cases are demonstrated and proved in [6].

1. When the tangents of both points are real then both input and output links can fully rotate, and the mechanism is a double-crank.

2. One pair of double point tangents is real and the other complex conjugate means that one on the input or output links is a crank while the other is a rocker. The double point corresponding to the complex conjugate tangents is always an *acnode*, or *hermit point*, and the link that is the rocker depends on which double point is the acnode.

3. When both pairs of tangents are complex conjugates then both double points are acnodes and the mechanism is a double rocker.

The *genus* of an algebraic curve is defined as the deficiency between the maximum number of double points for a curve of it's order less the actual number of double points the curve possesses [18]. While the algebraic properties of a planar algebraic curve will be discussed in greater detail in Section 3.6.2, we will hint at the material here. The maximum number of double points, $DP_{\max}$, a curve of order n can have is

$$DP_{\max} = \frac{1}{2}(n-1)(n-2). \tag{3.20}$$

Hence, a curve of order $n = 4$ can have a maximum of three double points. The algebraic I-O curve possesses only two as proved by the existence of only a pair common solutions to Equations (3.18), therefore it is always deficient by one. In other words, the genus of the algebraic I-O curve is 1.

The genus of a curve plays a very important role in the theory of curves [19, 20]. We can define the genus of an algebraic curve, $\mathcal{G}$, as the maximum number of possible double points, $DP_{\max}$, less the actual number, DP_{act} as an equation to make it easier to remember:

$$\mathcal{G} = DP_{\max} - DP_{\text{act}}. \tag{3.21}$$

If $\mathcal{G} = 0$ the curve possesses it's maximum number of double points, in other words $DP_{\text{act}} = DP_{\max}$, then the coordinates of any point on the curve can be expressed as rational algebraic functions of a single variable parameter. This means that an n-dimensional curve with $\mathcal{G} = 0$ can be parametrised and the coordinates may be expressed as rational algebraic functions of parameter t as

$$\begin{aligned} x_1 &= f_1(t) \\ x_2 &= f_2(t) \\ &\vdots \\ x_n &= f_n(t). \end{aligned}$$

If however the genus of the curve is $\mathcal{G} > 0$, then there is no way to parametrise the curve. Because the genus of the algebraic version of the I-O curve has genus $\mathcal{G} = 1$, it cannot be parametrised, and it is defined to be an *elliptic* curve [20]. This definition does not mean that the curve has the form of an ellipse, rather it means that the curve can be expressed, with a suitable change of variables, as an elliptic curve. In the plane, every elliptic curve with real coefficients can be put in the standard form

$$x_2^2 \quad = \quad x_1^3 + Ax_1 + B$$

for some real constants A and B.

3.2 Design Parameter Octahedron

In the projection of the design parameter space into the hyperplane $d = 1$, the eight linear factors in Equation (3.16) can be interpreted as the eight faces of a regular octahedron determined by the six vertices $V = (a, b, c)$: $V_1 = (1, 0, 0)$; $V_2 = (-1, 0, 0)$; $V_3 = (0, 1, 0)$; $V_4 = (0, -1, 0)$; $V_5 = (0, 0, 1)$; $V_6 = (0, 0, -1)$, see Figure 3.2.

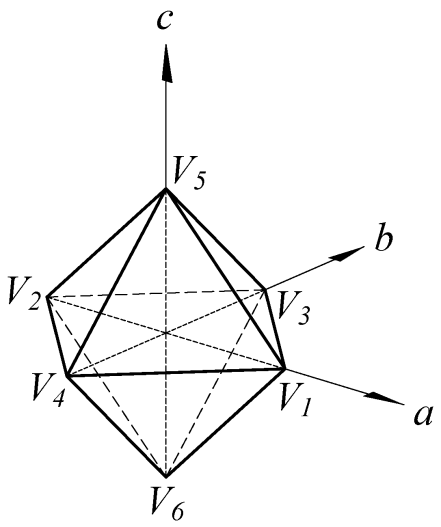

Figure 3.4. Design parameter octahedron.

Each face of the octahedron lies entirely in one of the eight quadrants in the parameter space. Considering the design parameter octahedron, four questions naturally arise.

1. What do the six vertices imply?
2. What is the significance of points on the octahedron edges?
3. What is the significance of points on the octahedron faces?
4. What is the significance of the location of a general point in the parameter space?

3.2.1 The Six Octahedron Vertices

With reference to Figure 3.4, each of the six octahedron vertices lie at the terminal ends of the design parameter space basis unit vectors, **a**, **b**, and **c**. They

comprise the six points $V_{1,2} = (\pm 1, 0, 0)$, $V_{3,4} = (0, \pm 1, 0)$, $V_{5,6} = (0, 0, \pm 1)$. Each vertex is the point common to the planes of four faces and represents a degenerate planar four-bar mechanism with no mobility because it contains two links of zero length and two links of unit length.

3.2.2 The Twelve Octahedron Edges

Again, referring to Figure 3.4, each of the twelve octahedron edges is the line in common with two octahedron faces excluding the vertices. Each edge lies entirely in one of eight design parameter sub-space coordinate planes. For example, the edge that lies in the coordinate plane spanned by the positive basis vectors **a** and **b** is the intersection of the face planes defined by the vertices $\{V_1, V_3, V_5\}$ and $\{V_1, V_6, V_3\}$. Each edge represents a degenerate four-bar mechanism with no mobility because it contains one link of zero length.

3.2.3 Points on the Eight Octahedron Faces

Because of the beautiful structure of the eight linear factors in Equation (3.16), it may be shown in a straightforward way that each of the linear factors defines one of eight planes containing one of the octahedron faces. In Euclidean space, E_3, a necessary and sufficient condition that four points, whose homogeneous point coordinates are $(x_0 : x_1 : x_2 : x_3)$, $(y_0 : y_1 : y_2 : y_3)$, $(z_0 : z_1 : z_2 : z_3)$ and $(w_0 : w_1 : w_2 : w_3)$, be coplanar is that [21, 22, 23]

$$\begin{vmatrix} x_0 & x_1 & x_2 & x_3 \\ y_0 & y_1 & y_2 & y_3 \\ z_0 & z_1 & z_2 & z_3 \\ w_0 & w_1 & w_2 & w_3 \end{vmatrix} = 0. \tag{3.22}$$

It follows that the plane determined by three distinct points has the equation

$$X_0x_0 + X_1x_1 + X_2x_2 + X_3x_3 = 0, \tag{3.23}$$

where the *plane coordinates* $[X_0 : X_1 : X_2 : X_3]$ are obtained by Grassmannian expansion [3, 23] of the matrix in Equation (3.22), giving

$$\begin{aligned} &\begin{vmatrix} y_1 & y_2 & y_3 \\ z_1 & z_2 & z_3 \\ w_1 & w_2 & w_3 \end{vmatrix} x_0 + \begin{vmatrix} y_0 & y_3 & y_2 \\ z_0 & z_3 & z_2 \\ w_0 & w_3 & w_2 \end{vmatrix} x_1 \\ &+ \begin{vmatrix} y_0 & y_1 & y_3 \\ z_0 & z_1 & z_3 \\ w_0 & w_1 & w_3 \end{vmatrix} x_2 + \begin{vmatrix} y_0 & y_2 & y_1 \\ z_0 & z_2 & z_1 \\ w_0 & w_2 & w_1 \end{vmatrix} x_3 = 0. \end{aligned} \tag{3.24}$$

Employing the Grassmannian expansion we obtain the equation of the plane containing the octahedron face defined by the vertices $\{V_1, V_6, V_3\}$ using their homogeneous coordinates: $V = (1 : a : b : c) \Rightarrow V_1 = (1 : 1 : 0 : 0)$, $V_6 = (1 : 0 : 0 : -1)$, $V_3 = (1 : 0 : 1 : 0)$. Using the determinants in Equation (3.24) and the three vertices reveals the corresponding plane coordinates as

$$[X_0 : X_1 : X_2 : X_3] \;=$$

$$\left[\begin{vmatrix} 1 & 0 & 0 \\ 0 & 0 & -1 \\ 0 & 1 & 0 \end{vmatrix} : \begin{vmatrix} 1 & 0 & 0 \\ 1 & -1 & 0 \\ 1 & 0 & 1 \end{vmatrix} : \begin{vmatrix} 1 & 1 & 0 \\ 1 & 0 & -1 \\ 1 & 0 & 0 \end{vmatrix} : \begin{vmatrix} 1 & 0 & 1 \\ 1 & 0 & 0 \\ 1 & 1 & 0 \end{vmatrix}\right] = [1 : -1 : -1 : 1].$$

Hence, the plane equation containing face $\{V_1, V_6, V_3\}$ can be expressed as

$$1 - a - b + c \;=\; 0. \tag{3.25}$$

When the coordinates in Equation (3.25) are homogenised, the relation can be expressed as

$$a + b - c - d \;=\; 0. \tag{3.26}$$

Thus, the plane equation determined by the three vertices $\{V_1, V_6, V_3\}$ is precisely the linear factor C_1 in Equation (3.16). The remaining seven linear factors in Equation (3.16) are, similarly, the plane equations for the seven other octahedron faces. If a point in the design parameter space satisfies Equation (3.26), then it lies in the plane of the face spanned by the three vertices $\{V_1, V_6, V_3\}$, and the corresponding mechanism has link lengths constrained by the relation $a + b = c + d$. Depending on the lengths of the individual links satisfying this relation the resulting mechanism can be a double crank, double rocker, or crank rocker, and can have up to two folding configurations and assembly modes [6, 24].

Similarly, points in the planes of the faces spanned by vertices $\{V_2, V_5, V_3\}$ and by vertices $\{V_1, V_5, V_4\}$ lead to the plane equations

$$1 + a - b - c = 0 \quad \text{and} \quad 1 - a + b - c = 0,$$

which correspond to the linear factors A_1 and D_1 respectively, when the coordinates are homogenised giving

$$a - b - c + d = 0 \quad \text{and} \quad a - b + c - d = 0.$$

Points laying in the planes of these two faces correspond to linkages with link lengths constrained by the relations $a + d = b + c$ and $a + c = b + d$. Again,

depending on the lengths, the resulting mechanisms can be a double-crank, double-rocker, or crank-rocker, and can have up to two folding configurations and assembly modes. However, points in the planes spanned by the remaining five faces, corresponding to linear factors A_2, B_1, B_2, C_2, and D_2 represent linkages with zero finite mobility because either the sum of all the link lengths is identically zero, or one link length is equal to the sum of the lengths of the remaining three.

3.2.4 A General Point in the Design Parameter Space

The location of a single point in the design parameter space is a specific planar $4R$ whose link lengths satisfy Equation (3.16). The values of the link lengths are directed distances, and hence can have positive or negative values. Clearly, if one of the lengths is identically zero, then the resulting $3R$ linkage is a structure.

The absolute values of the link lengths identified with Equation (3.16) lead to an alternate form of the classification scheme for planar $4R$ linkages first presented in [24] and later refined in [25], and hence to an expression for the Grashof condition [26]. Recall that a Grashof four-bar linkage is one in which the sum of the lengths of the longest and shortest links is less than the sum of the lengths of the other two links. A Grashof planar $4R$ mechanism may contain at least one link that can fully rotate, or both input and output angles rock in a range between 0 and π if

$$l + s \quad < \quad p + q, \tag{3.27}$$

where l and s refer to the lengths of the longest and shortest links, while p and q are the lengths of the two intermediate links.

There are three possibilities. The first four are the possible Grashof planar $4R$ mechanisms for which the following relations, stated without proof, are valid.

1. The four possible Grashof planar $4R$ mechanisms.
   (a) Link a is a crank if it is the shortest link, and the output link b is a rocker.
   (b) Link b is a crank if it is the shortest link, and the input link a is a rocker.
   (c) If the relatively non-moving link, the base, is the shortest link, then both the input and output links a and b are cranks.
   (d) If the coupler is the shortest link, then both the input and output links a and b are rockers.

2. If $l + s > p + q$ then there are four different inversions of double rocker mechanisms that result, which are all non-Grashof linkages.

3. If $l + s = p + q$ the mechanism is known as a *change-point mechanism*, because it can fold. These linkages are also known as folding linkages. These are also non-Grashof linkages. There are two special cases.

   (a) If all four links are of equal length, $a = b = c = d$, the change-point linkage is known as a *parallelogram linkage*. All four inversions can be double cranks if they can stay in the same branch of the coupler curve, see Section 3.6.

   (b) The *deltoid linkage* is the other special case where two equal length short links are connected to two equal length long links.

3.2.5 Continuous Sets of Points in the Design Parameter Space

Planar four-bar linkages however are not exclusively jointed with R-pairs, they often contain P-pairs. However, four-bar mechanisms containing more than two P-pairs cannot move the coupler in general plane motion, rather they can only generate translations and hence are not considered here. Any kinematic inversion of an $RRRP$ linkage will possess one variable link length and one variable joint angle, typically called a *slider-crank*, see Figure 3.5. Hence the roles of fixed constant and variable in Equation 3.16 can be reassigned to generate a function of the form $b = f(u)$, for example. The important thing to note is that the same IO equation can be used for kinematic synthesis! The resulting mechanism however, will not be represented by a single point in the design parameter space. Rather, it will be represented by a line parallel to the basis vector direction representing the variable link length. The length of the line will be determined by the extremities of the slider translation. This will be interesting to investigate in function generation optimisation problems and is, at the moment, an open research problem.

The kinematic inversions of the *elliptic-trammel* $PRRP$ linkage are the $RRPP$ and $RPPR$ linkages known as the *Scotch yoke* and *Oldham's coupling*, respectively. These linkages possess two variable link lengths. It turns out that Equation 3.16 can also be used for function generation synthesis of linkages possing two R- and two P-pairs. We believe this to be remarkable! Again, the roles of fixed constant and variable are reassigned. In this case the function generation synthesis problem can be modelled with Equation 3.16 to generate functions of

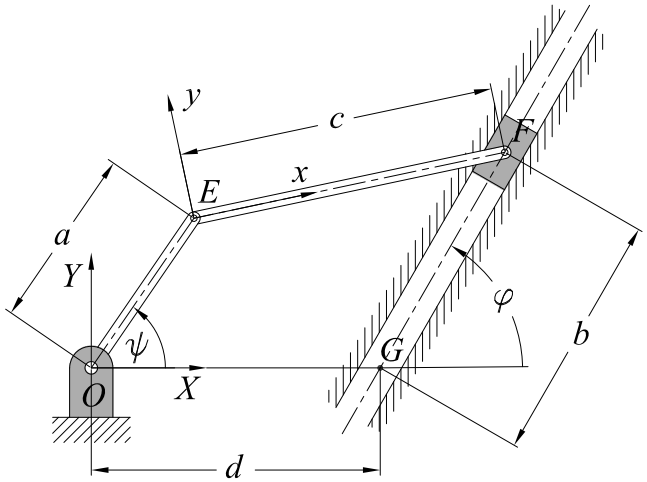

Figure 3.5: An $RRRP$ slider-crank.

the form $b = f(a)$, while the angles represented by u and v are now constants that are identified in the synthesis. In the design parameter space the resulting mechanism will be represented by a curve that is the approximated functional relationship between lengths a and b over the desired maximum input-output range.

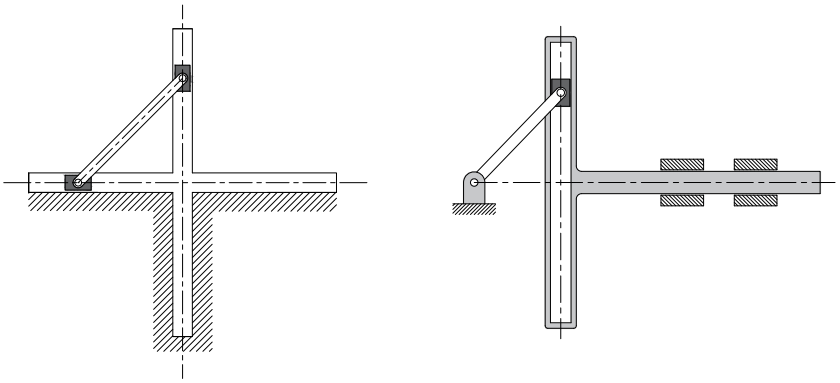

(a) Elliptical trammel, $PRRP$. (b) Scotch yoke, $RRPP$.

Figure 3.6: Kinematic inversions of the elliptical trammel.

The elliptical trammel is illustrated in Figure 3.6 (a). It consists of two P-pairs with perpendicular longitudinal axes of symmetry and a coupler which is attached to the sliders by R-pairs at fixed positions along the coupler. As the

P-pairs move back and forth, each along its channel, the points of the coupler move in elliptical paths. The semi-major and semi-minor axes of the ellipse have lengths equal to the distances from the coupler point to each of the two R-pair centres. The elliptical trammel was known in antiquity and is frequently called *the trammel of Archimedes* [27].

The Scotch yoke is illustrated in Figure 3.6 (b). The Scotch yoke, also known as slotted link mechanism, is an $RRPP$ linkage that generates reciprocating motion, converting the rotational motion of a ground fixed R-pair into reciprocating translational motion, or vice versa. The first P-pair is directly coupled to a sliding yoke with a slot that engages an R-pair on the rotating link. The location of the first P-pair versus time is a sine wave of constant amplitude, and constant frequency given a constant rotational speed.

The Oldham coupling, illustrated in Figure 3.7, is an $RPPR$ kinematic chain. It is used to connect two parallel shafts whose axes are at a small distance apart. Two flanges, each having a rectangular slot, are keyed, one on each shaft. The two flanges are positioned such that, the slot in one is at right angle to the slot in the other. To make the coupling, a circular disc with two rectangular projections on either side and at right angle to each other, is placed between the two flanges. During motion, the central disc, while turning, slides in the slots of the flanges. Power transmission takes place between the shafts, because of the positive connection between the flanges and the central disc [28].

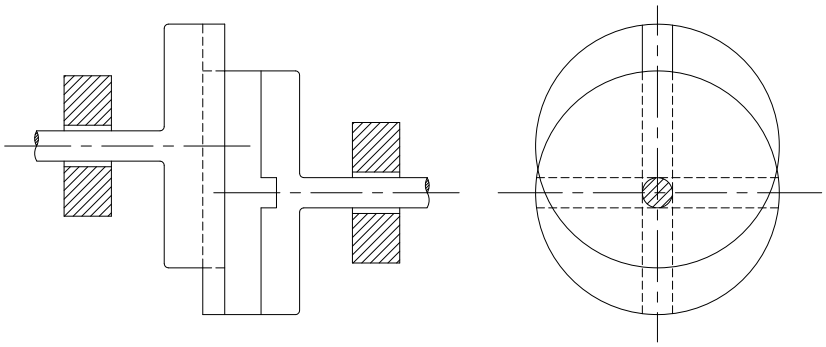

Figure 3.7: The Oldham coupling, $RPPR$.

3.3 Classification of Planar 4R Mechanisms

In this section we present a classification of planar $4R$ mechanisms that builds on the one originally proposed in [24]. First we consider the angular limits

on the input and output angles ψ and φ, if they exist. Next, we consider the implications of the vanishing of the linear factors A_1, C_1 and D_1 from Equation (3.16). Finally, the signed numerical values of the same linear factors A_1, C_1 and D_1 are used, together with the limits on the input and output angles to classify the mechanisms according to the associated mobility constraints. In this way, this classification technique is additionally an alternate way to evaluate the Grashof condition.

3.3.1 Input Link, a.

The limits of angular displacement for the input link, a, if they exist, can be determined using the law of cosines and the two triangles formed by the lengths a and d when the coupler and output link align, giving lengths $c-b$ and $c+b$, respectively, see Figure 3.10. In order for $\psi_{\min}$ and $\psi_{\max}$ to exist, then

$$-1 \leq \cos(\psi) \leq 1. \tag{3.28}$$

It can be shown using the methods in [25, 24] that the conditions leading to

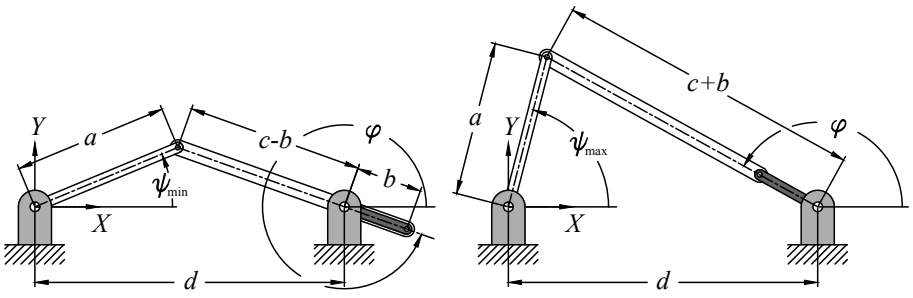

Figure 3.10: The angular limits of the output link, if they exist, are $\psi_{\min/\max}$.

$-1 < \cos(\psi) > 1$ can be expressed as the product of two linear factors from Equation (3.16). The fist product concerns the existence of $\psi_{\min}$:

$$(a+b-c-d)(a-b+c-d) \quad > \quad 0 \quad \text{(i.e. } C_1 D_1 \; > \; 0). \tag{3.29}$$

If this condition is satisfied, then both factors must be either positive or negative, and the input link has no $\psi_{\min}$. This implies that the input link can rotate through $\psi = 0$ reaching angles below the line joining the centres of the two ground fixed R-pairs. If this condition is not satisfied then one of either C_1 or

D_1 is negative and $\psi_{\min}$ may be computed, using the upper sign $(c-b)^2$, as[1]

$$\psi_{\substack{\min \\ \max}} = \cos^{-1}\left(\frac{a^2+d^2-(c\mp b)^2}{2ad}\right). \tag{3.30}$$

Referring again to Figure 3.10, the second product concerns the existence of $\psi_{\max}$, and can be expressed as:

$$(a-b-c+d)(a+b+c+d) < 0 \quad (\text{i.e. } A_1B_2 < 0). \tag{3.31}$$

If this condition is satisfied then $\psi_{\max}$ does not exist, and the input link can rotate through π. Since B_2 must always be positive, this condition simplifies to

$$a+d < b+c. \tag{3.32}$$

If the condition in Equation (3.31) is not satisfied, then it must be that $a+d \geq b+c$, and $\psi_{\max}$ may be computed using the lower sign $(c+b)^2$ in Equation (3.30).

The classification, as in [24], uses the observation that if $C_1D_1 > 0$ and $A_1 < 0$ then neither $\psi_{\min}$ nor $\psi_{\max}$ exist, and the input link is a fully rotatable crank and therefore the link lengths must satisfy the Grashof condition. If $C_1D_1 > 0$ while $A_1 \geq 0$ then $\psi_{\max}$ exists, but not $\psi_{\min}$, and the input link is a 0-rocker because it rocks through 0 between the $\pm\psi_{\max}$ limits. If $C_1D_1 \leq 0$ while $A_1 < 0$ then $\psi_{\min}$ exists, but not $\psi_{\max}$, and the input link is a π-rocker because it rocks through π between the $\pm\psi_{\min}$ limits. Alternately, if $C_1D_1 \leq 0$ and $A_1 \geq 0$ then both $\psi_{\min}$ and $\psi_{\max}$ exist and the input link is a rocker which can pass through neither 0 nor π and rocks in one of two sperate ranges: $\psi_{\min} \leq \psi_{\max}$; or $-\psi_{\max} \leq -\psi_{\min}$.

3.3.2 Output Link, b.

The limits of angular displacement for the output link, b, if they exist, can be determined using the law of cosines and the two triangles formed by the lengths b and d when the coupler and input link align, giving lengths $c+a$ and $c-a$, respectively, see Figure 3.11. Note that φ in this case is an exterior angle, and the corresponding angle used in the law of cosines is $\pi-\varphi$ necessitating as sign change: $-\cos(\pi-\varphi) = \cos(\varphi)$. In order for $\varphi_{\min}$ and $\varphi_{\max}$ to exist, then

$$-1 \leq \cos(\varphi) \leq 1. \tag{3.33}$$

The conditions leading to $-1 > \cos(\varphi) > 1$ can be expressed as the products

[1] Note that $\cos(\psi)$ returns the same value for $\pm\psi$. Hence, the $\cos^{-1}$ function leads to two limiting values of $\pm\psi_{\min}$ and $\pm\psi_{\max}$, one for each of the *elbow up* and *elbow down* assembly modes of the linkage.

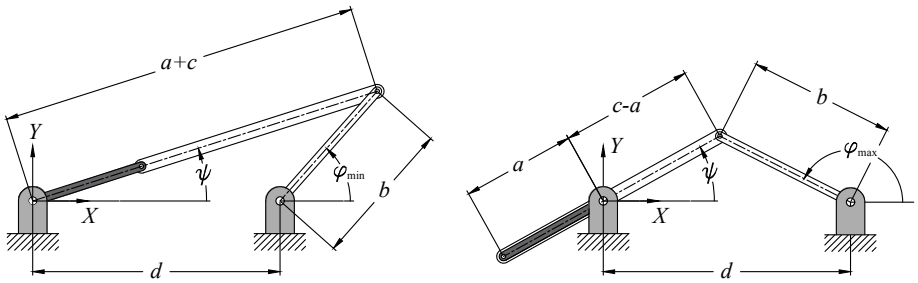

Figure 3.11: The angular limits of the output link, if they exist, are $\varphi_{\min/\max}$.

of two linear factors from Eq. (3.16). If $\varphi_{\min}$ does not exist then a and c can't align and:

$$(a-b+c-d)(a+b+c+d) \;>\; 0 \quad \text{(i.e. } D_1 B_2 \;>\; 0\text{)}. \tag{3.34}$$

Since B_2 is always positive, then in order to satisfy Eq. (3.34) D_1 must also be positive. This leads to the simpler expression for the condition in Eq. (3.34):

$$a+c \;>\; b+d. \tag{3.35}$$

If this condition is satisfied, then $\varphi_{\min}$ does not exist and the output link can rotate through $\varphi = 0$ reaching angles below the line joining the centres of the two ground fixed R-pairs. When this condition is not satisfied then D_1 is either identically zero or negative meaning that $\varphi_{\min}$ exists and may be computed using the upper sign $(a+c)^2$ in Equation (3.36) as

$$\varphi_{\substack{\min \\ \max}} \;=\; \cos^{-1}\left(\frac{(a \pm c)^2 - (b^2+d^2)}{2bd}\right). \tag{3.36}$$

Referring again to Figure 3.11, the second product concerns the existence of $\varphi_{\max}$, and can be expressed as:

$$(a-b-c+d)(a+b-c-d) \;<\; 0 \quad \text{(i.e. } A_1 C_1 \;<\; 0\text{)}. \tag{3.37}$$

If this condition is satisfied then $\varphi_{\max}$ does not exist, and the output link can rotate through π. Satisfying this condition requires that one factor is positive while the other is negative. If the condition in Equation (3.37) is not satisfied, then it must be that A_1 and C_1 are either both positive or negative. In this case $\varphi_{\max}$ may be computed using the lower sign $(a-c)^2$ in Equation (3.36).

Again, following [24], the Grashof condition for this case is $A_1 C_1 < 0$ and $D_1 > 0$. Using these conditions as indicators, the output link can also be a crank, a 0-rocker, a π-rocker, or a rocker restricted to one of the two separate ranges bounded by 0 and π: $\varphi_{\min} \leq \varphi_{\max}$; or $-\varphi_{\max} \leq -\varphi_{\min}$.

3.3.3 Implications of Vanishing Linear Factors.

The remaining conditions to consider are if any one, or more, of the three factors are identically zero. Consider the following zeros:

$$\begin{aligned} A_1 = 0 \quad &\Rightarrow \quad a - b - c + d = 0 \quad \Rightarrow \quad a + d = b + c; \\ C_1 = 0 \quad &\Rightarrow \quad a + b - c - d = 0 \quad \Rightarrow \quad a + b = c + d; \\ D_1 = 0 \quad &\Rightarrow \quad a - b + c - d = 0 \quad \Rightarrow \quad a + c = b + d. \end{aligned}$$

If only one of $A_1 = 0$, $C_1 = 0$, or $D_1 = 0$, then the mechanism is a point on one of the planes containing the faces of the octahedron spanned by either vertices $\{V_2, V_5, V_3\}$, $\{V_1, V_6, V_3\}$, or $\{V_4, V_1, V_5\}$, respectively. In each case, the linkage has a single folding configuration.

If two of the factors are identically zero, then the mechanism is represented by a point that lies on the line of intersection of the two corresponding faces, which is never an octahedron edge for pairs of these three faces. In this case, the linkage has two folding configurations because of the equality in length of two different sums of pairs of link lengths.

Finally, if all three factors are simultaneously identical to zero, the corresponding mechanism is represented by the point common to the planes of all three associated octahedron faces. It is a simple matter to show this leads to a third order equation with only one solution: $a = b = c = d$. In the design parameter space normalised with $d = 1$, this means the point $(1, 1, 1)$, a rhombus linkage possessing three folding configurations.

3.3.4 Summary of Implications For Different Values of the Three Linear Factors A_1, C_1, D_1.

A summary of the meanings for the different values of the three linear factors from Equation (3.16) is itemised in the following four subsections.

3.3.4.1 Input Link a and Input Angle ψ

1. If $C_1 D_1 > 0 \;\Rightarrow\; \psi_{\min}$ does not exist and ψ passes through 0.
2. If $C_1 D_1 \leq 0 \;\Rightarrow\; \psi_{\min}$ exists and is computed using the upper sign $(c - b)^2$ in Equation (3.30).
3. If $A_1 < 0 \;\Rightarrow\; \psi_{\max}$ does not exist and ψ passes through π.
4. If $A_1 \geq 0 \;\Rightarrow\; \psi_{\max}$ exists and is computed using the lower sign $(c + b)^2$ in Equation (3.30).

3.3.4.2 Implications for the Range of Motion of Input Link a

1. If $A_1 < 0$ and $C_1 D_1 > 0$ $\Rightarrow$ input link a is a crank.
2. If $A_1 < 0$ and $C_1 D_1 \leq 0$ $\Rightarrow$ input link a is a π-rocker: $\psi_{\min}$ exists but link a passes through π.
3. If $A_1 \geq 0$ and $C_1 D_1 > 0$ $\Rightarrow$ input link a is a 0-rocker: $\psi_{\max}$ exists but link a passes through 0.
4. If $A_1 \geq 0$ and $C_1 D_1 \leq 0$ $\Rightarrow$ input link a is a rocker: both $\psi_{\min}$ and $\psi_{\max}$ and input link a rocks over some region in the range between $\pi \leq \psi \geq 0$.

3.3.4.3 Output Link b and Output Angle φ

1. If $D_1 > 0$ $\Rightarrow$ $\phi_{\min}$ does not exist and ϕ passes through 0.
2. If $D_1 \leq 0$ $\Rightarrow$ $\phi_{\min}$ exists and is computed using the upper sign $(a+c)^2$ in Equation (3.36).
3. If $A_1 C_1 < 0$ $\Rightarrow$ $\phi_{\max}$ does not exist and ϕ passes through π.
4. If $A_1 C_1 \geq 0$ $\Rightarrow$ $\phi_{\max}$ exists and is computed using the lower sign $(a-c)^2$ in Equation (3.36).

3.3.4.4 Implications for the Range of Motion of Output Link b

1. If $A_1 C_1 < 0$ and $D_1 > 0$ $\Rightarrow$ output link b is a crank.
2. If $A_1 C_1 < 0$ and $D_1 \leq 0$ $\Rightarrow$ output link b is a π-rocker: $\phi_{\min}$ exists but link b passes through π.
3. If $A_1 C_1 \geq 0$ and $D_1 > 0$ $\Rightarrow$ output link b is a 0-rocker: $\phi_{\max}$ exists but link b passes through 0.
4. If $A_1 C_1 \geq 0$ and $D_1 \leq 0$ $\Rightarrow$ output link b is a rocker: both $\phi_{\min}$ and $\phi_{\max}$ and output link b rocks over some region in the range between $\pi \leq \phi \geq 0$.

3.3.5 Classification

Any planar $4R$ linkage can be classified according to the values of the three linear factors A_1, C_1, and D_1 which can each either be positive, identically zero, or negative. Using the criteria from above the linkage type can be classified according to it's link lengths. There are 27 distinct permutations positive and negative signs, taken three at a time, and all the corresponding 27 possible mechanisms are listed in Table 3.1.

#	A_1	C_1	D_1	Input a	Output b	#	A_1	C_1	D_1	Input a	Output b
1	+	+	+	0-rocker	0-rocker	15	0	0	-	crank	π-rocker
2	+	+	0	0-rocker	0-rocker	16	0	-	+	π-rocker	crank
3	+	+	-	rocker	rocker	17	0	-	0	crank	crank
4	+	0	+	0-rocker	crank	18	0	-	-	crank	π-rocker
5	+	0	0	0-rocker	crank	19	-	+	+	crank	crank
6	+	0	-	0-rocker	π-rocker	20	-	+	0	crank	crank
7	+	-	+	rocker	crank	21	-	+	-	π-rocker	π-rocker
8	+	-	0	0-rocker	crank	22	-	0	+	crank	crank
9	+	-	-	0-rocker	π-rocker	23	-	0	0	crank	crank
10	0	+	+	crank	crank	24	-	0	-	crank	π-rocker
11	0	+	0	crank	crank	25	-	-	+	π-rocker	0-rocker
12	0	+	-	π-rocker	π-rocker	26	-	-	0	crank	0-rocker
13	0	0	+	crank	crank	27	-	-	-	crank	rocker
14	0	0	0	crank	crank						

Table 3.1: Classification of all 27 possible planar $4R$ linkages. Shaded cells satisfy the Grashof condition.

We now briefly revisit the Grashof condition, stated by Equation (3.27). Because of the conditions on the numerical value of the three factors A_1, C_1, and D_1 in Table 3.1 it is to be seen that the Grashof condition can be restated in terms of the product of the numerical values, without explicit regard to link lengths, as

$$A_1 C_1 D_1 \quad < \quad 0. \tag{3.38}$$

Consider the Grashof double-rocker listed in Element 3 of Table3.1. Because $A_1 > 0$ and $C_1 D_1 < 0$, the input angle rocks in limits that are limited by $\pi < \psi > 0$, and because $A_1 C_1 > 0$ while $D_1 < 0$ the output angle also rocks in

limits that are limited by $\pi < \varphi > 0$, and hence the linkage is a Grashof double-rocker. The Grashof rocker-crank in Element 7 of the table is so determined because $A_1 > 0$ and $C_1 D_1 < 0$ the input angle rocks in limits that are limited by $\pi < \psi > 0$, however the output link is a fully rotatable crank because $A_1 C_1 < 0$ and $D_1 < 0$. The Grashof double-crank listed in Element 19 is so because $A_1 < 0$ and $C_1 D_1 > 0$, meaning that the input link a is a crank, and because $A_1 C_1 < 0$ while $D_1 > 0$, so the output link b is also a crank. Finally, Element 27 is a Grashof crank-rocker because $A_1 < 0$ and $C_1 D_1 > 0$, meaning that the input link a is a crank, while $A_1 C_1 > 0$ and $D_1 < 0$ so the output link b is a rocker that rocks in limits that are limited by $\pi < \varphi > 0$.

3.4 Coupler Angle

The goal of this section is to obtain an expression for the angle α the coupler c makes with respect to the input link a in terms of the input and output angles, ψ and φ, and the link lengths a, b, and d, see Figure 3.12.

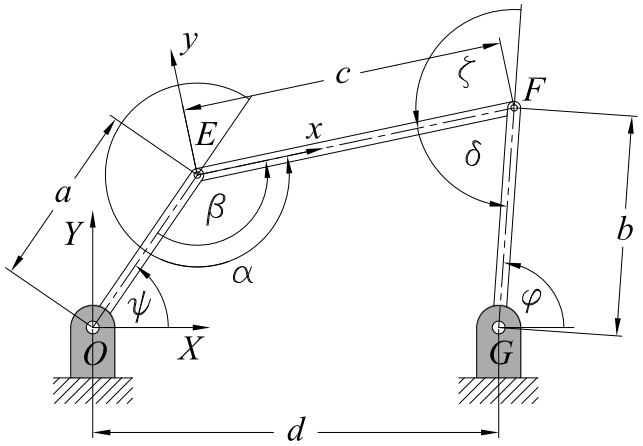

Figure 3.12: 4R four-bar mechanism parameters.

This material is partly based on the material presented in [25]. Let α denote the angle of the coupler c measured about E relative to the input link a. Hence, the angle $\psi + \alpha$ measures the angle the coupler c makes with respect to the X-axis of the relatively fixed coordinate system centred at O. The coordinates of F can be defined in terms of α as

$$\begin{bmatrix} F_X \\ F_Y \end{bmatrix} = \begin{bmatrix} a\cos\psi + c\cos(\psi + \alpha) \\ a\sin\psi + c\sin(\psi + \alpha) \end{bmatrix}. \tag{3.39}$$

But, the coordinates of F can also be defined in terms of the output link b as

$$\begin{bmatrix} F_X \\ F_Y \end{bmatrix} = \begin{bmatrix} d + b\cos\varphi \\ b\sin\varphi \end{bmatrix}. \tag{3.40}$$

Equation Equations (3.39) and (3.40) yields the kinematic closure equations for the four-bar linkage:

$$a\cos\psi + c\cos(\psi+\alpha) = d + b\cos\varphi, \tag{3.41}$$

$$a\sin\psi + c\sin(\psi+\alpha) = b\sin\varphi. \tag{3.42}$$

For any value of the input angle ψ we can write

$$\cos(\psi+\alpha) = \frac{d + b\cos\varphi - a\cos\psi}{c},\ \sin(\psi+\alpha) = \frac{b\sin\varphi - a\sin\psi}{c}. \tag{3.43}$$

We can solve Equation (3.43) for α revealing

$$\alpha = \tan^{-1}\left(\frac{b\sin\varphi - a\sin\psi}{d + b\cos\varphi - a\cos\psi}\right) - \psi. \tag{3.44}$$

3.5 Performance Metrics

Various angles and ratios of a four-bar mechanism act as performance metrics that can be used to evaluate how well a mechanism performs the task it is intended for, or to compare the performance of different linkages at carrying out the same task. While there is no single performance metric, or index of merit [28] for all mechanisms, several have emerged as particularly useful. The *transmission angle* between the coupler c and output link b, ζ in Figures 3.12 and 3.13, is a standard four-bar mechanism performance metric that can be used as a measure of the *mechanical advantage* and *velocity ratio* of a particular linkage. These three metrics will be discussed in the following two subsections.

3.5.1 Transmission Angle

If the only external loads on linkage are generated by torques on the input and output links, then the forces $\mathbf{F}_E$ and $\mathbf{F}_F$ acting on the coupler at the centres of the revolute joints connecting it to the input and output links must act in opposite directions acting along the line connecting the two moving joint centres. Hence, in general only a component of force $\mathbf{F}_F$ is transferred to the output link as output torque via the coupler depending on the transmission angle ζ. The component of $\mathbf{F}_F$ transmitted to the output link as torque is proportional to

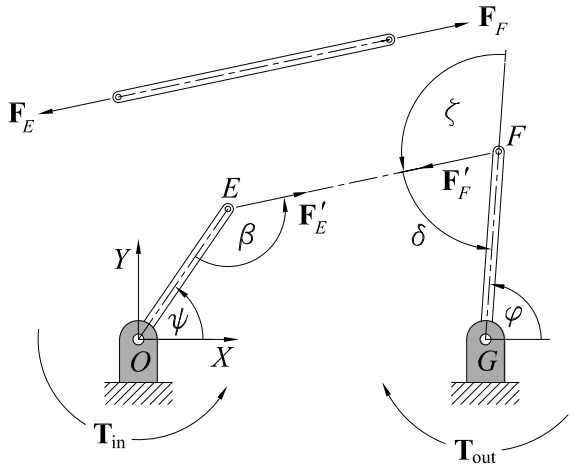

Figure 3.13: 4R four-bar mechanism parameters.

$\sin\zeta$. The component proportional to $\cos\zeta$ is transferred to the centre of the ground fixed revolute joint at G and must be absorbed as a reaction force.

It is useful to have the transmission angle ζ expressed in terms of the input angle ψ. To do this we can equate the cosine laws for the triangles $\triangle OGE$ and $\triangle GFE$ along the diagonal EG of the quadrangle formed by the revolute joint centres $OGFE$. Referring to Figure 3.13, because ζ is an exterior angle this gives

$$(|\mathbf{E}-\mathbf{G}|)^2 = d^2 + a^2 - 2ad\cos\psi = b^2 + c^2 + 2bc\cos\zeta. \tag{3.45}$$

Solving for the transmission angle ζ yields

$$\zeta = \cos^{-1}\left(\frac{d^2 + a^2 - b^2 - c^2 - 2ad\cos\psi}{2bc}\right). \tag{3.46}$$

3.5.2 Mechanical Advantage and Velocity Ratio

Consider Figures 3.12 and 3.13 once again. If friction and inertia forces are small compared to the actuation forces then the power supplied to the input link a is the negative of the power applied to the output link b by the load. Since power can be defined as the inner (dot) product of torque and angular velocity vectors it must be that

$$\mathbf{T}_{\text{in}} \cdot \dot{\boldsymbol{\psi}} \quad = \quad -\mathbf{T}_{\text{out}} \cdot \dot{\boldsymbol{\varphi}}. \tag{3.47}$$

We can consider only the magnitudes of these vectors and re-express this relation as the following equivalent ratios:

$$\frac{T_{\text{out}}}{T_{\text{in}}} = -\frac{\dot{\psi}}{\dot{\varphi}}. \tag{3.48}$$

The first ratio in Equation (3.48) is the *mechanical advantage* of the linkage, which is equivalent to the negative reciprocal of the *velocity ratio*. The velocity ratio in Equation (3.48) can be expressed in terms of the two angles δ and β illustrated in Figure 3.12. Since δ is $\pi - \zeta$ we additionally have

$$\frac{T_{\text{out}}}{T_{\text{in}}} = -\frac{\dot{\psi}}{\dot{\varphi}} = -\frac{b \sin \delta}{a \sin \beta}. \tag{3.49}$$

Equation (3.49) shows that the mechanical advantage approaches infinity when the angle β approaches 0 or π. These configurations are called *toggle* configurations, and are illustrated in Figure 3.11. The two toggle configurations for the linkage in Figure 3.11 correspond to $\beta = 0$ and $\beta = \pi$. Moreover, Equation (3.49) also shows that issues arise when $\delta \to 0$ and $\delta \to \pi$. These two extremes for the transmission angle correspond to when $\zeta \to \pi$ and $\zeta \to 0$. In these configurations the mechanical advantage of the linkage becomes very small, and then even a very small amount of friction or misalignment will cause the mechanism to jam or lock. Hence, a design rule-of-thumb is that the best four-bar linkage will have a transmission angle which deviates from a right angle by the smallest amount [28].

3.6 Coupler Curves

The point equation for the coupler curve of a selected coupler point which is generated by a planar $4R$ mechanism that is presented here is largely based on the way it was originally derived in [29] and reported in [18], and subtly modified in [25]. Referring to Figure 3.14, the ground fixed stationary reference coordinate system has it's origin O at the centre of the left ground fixed R-pair and uses coordinates (X, Y). Let the coordinate system that moves with the coupler be centred at E, with x-axis on the line between E and F. Let the coordinates of any particular coupler reference point C be (x_C, y_C). Since the coupler angle α is a function of the input angle ψ we will express the equation of the coupler curve that point C traces as ψ changes in terms of the input angle all expressed in the non-moving coordinate system. Since the location of point C has constant coordinates (x_C, y_C) in the moving coordinate system, we

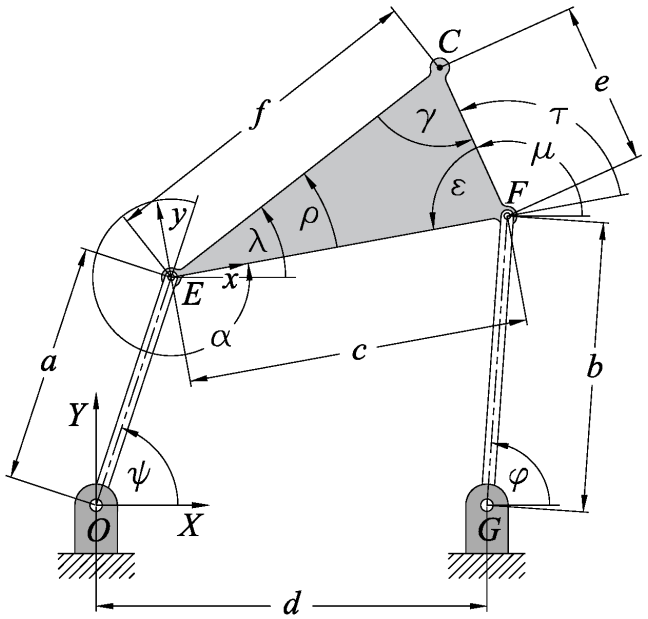

Figure 3.14: 4R four-bar point coupler curve parameters.

can always transform these coordinates to the non-moving frame coordinates (X_C, Y_C) with the coordinate transformation

$$\begin{bmatrix} 1 \\ X_C(\psi) \\ Y_C(\psi) \end{bmatrix} = \begin{bmatrix} 0 & 0 & 1 \\ \cos(\psi+\alpha) & -\sin(\psi+\alpha) & a\cos\psi \\ \sin(\psi+\alpha) & \cos(\psi+\alpha) & a\sin\psi \end{bmatrix} \begin{bmatrix} 1 \\ x_C \\ y_C \end{bmatrix}. \quad (3.50)$$

The coupler geometry is fixed with the angle at the coupler reference point C between sides f and e indicated by the constant angle γ. Hence, by eliminating ψ from the equation, we can obtain a quasi-algebraic form of the coupler curve. However, the equation is still essentially transcendental in terms of $\cos\gamma$ and $\sin\gamma$, so we call it quasi-algebraic. We will define the coordinates of the coupler point C is two ways. Let the coupler triangle $\triangle CEF$ in Figure 3.14 have lengths c, e and f, where e and f are determined by the choice of coupler point C. These two sides are determined by

$$f = |\mathbf{C}-\mathbf{E}| = (x_C^2 + y_C^2)^{\frac{1}{2}}, \quad \text{and} \quad e = |\mathbf{C}-\mathbf{F}| = \left((x_C - c)^2 + y_C^2\right)^{\frac{1}{2}}. \quad (3.51)$$

The angle λ is defined in the non-moving frame centred at O as the angle that side f makes with respect to the X-axis, counter-clockwise being positive, while

the angle μ is the angle between the X-axis and side e. We therefore write

$$\mathbf{C}-\mathbf{E}=\begin{bmatrix}1\\ f\cos\lambda\\ f\sin\lambda\end{bmatrix},\quad\text{and}\quad\mathbf{C}-\mathbf{F}=\begin{bmatrix}1\\ e\cos\mu\\ e\sin\mu\end{bmatrix}. \tag{3.52}$$

Now de-homogenise and rearrange Equations (3.52) to isolate $\mathbf{E}$ and $\mathbf{F}$:

$$\mathbf{E}=\begin{bmatrix}X_C-f\cos\lambda\\ Y_C-f\sin\lambda\end{bmatrix},\quad\text{and}\quad\mathbf{F}=\begin{bmatrix}X_C-e\cos\mu\\ Y_C-e\sin\mu\end{bmatrix}. \tag{3.53}$$

Substitute these results into the identities defined in the fixed frame

$$\mathbf{E}\cdot\mathbf{E}=a^2,\quad\text{and}\quad(\mathbf{F}-\mathbf{G})\cdot(\mathbf{F}-\mathbf{G})=b^2.$$

The first dot product gives

$$\mathbf{E}\cdot\mathbf{E}\;=\;(X_C-f\cos\lambda)^2+(Y_C-f\sin\lambda)^2\;=\;a^2.$$

After collecting terms and using the identity $\cos^2\lambda+\sin^2\lambda=1$, and rearranging the terms this simplifies to

$$\mathbf{E}\cdot\mathbf{E}\;=\;X_C^2+Y_C^2-2fX_C\cos\lambda-2fY_C\sin\lambda+f^2\;=\;a^2. \tag{3.54}$$

Since our fixed coordinate system is selected such that the X-axis is directed from point O to point G, with the origin located at O, the difference of the two vectors in the second dot product is

$$\mathbf{F}-\mathbf{G}\;=\;\begin{bmatrix}X_C-e\cos\mu-d\\ Y_C-e\sin\mu\end{bmatrix}.$$

Using the same approach, the second dot product simplifies to

$$\begin{aligned}(\mathbf{F}-\mathbf{G})\cdot(\mathbf{F}-\mathbf{G})\;=\;&X_C^2+Y_C^2-2eX_C\cos\mu-2eY_C\sin\mu+\\ &2de\cos\mu-2dX_C+d^2+e^2\;=\;b^2.\end{aligned} \tag{3.55}$$

The next step is to eliminate the variable angle μ from Equation (3.55) by observing in Figure 3.14 that

$$\mu\;=\;\gamma+\lambda$$

and substituting into Equation (3.55). The addition identities for sine and cosine functions

$$\begin{aligned}\cos(\gamma+\lambda)&=\cos\gamma\cos\lambda-\sin\gamma\sin\lambda,\\ \sin(\gamma+\lambda)&=\cos\gamma\sin\lambda+\sin\gamma\cos\lambda,\end{aligned}$$

are used to separate the angle functions, and after rearranging the terms as in Equation (3.55) gives

$$\begin{aligned} X_C^2 + Y_C^2 \; - \; & 2e\left((X_C - d)\cos\gamma + Y_C \sin\gamma\right)\cos\lambda \; - \\ & 2e\left(Y_C\cos\gamma + (d - X_C)\sin\gamma\right)\sin\lambda + d^2 + e^2 - 2X_C d \;\; = \;\; b^2. \end{aligned} \tag{3.56}$$

The next step towards obtaining the quasi-algebraic point coupler curve expressed in the non-moving coordinate system in terms of X_C and Y_C is to linearly solve Equations (3.54) and (3.56) for $\cos\lambda$ and $\sin\lambda$ using Cramer's rule [30].

To apply Cramer's rule to this system of equations, the equations must be in the vector-matrix form $\mathbf{Ax} = \mathbf{b}$. Recall that if $\mathbf{Ax} = \mathbf{b}$ represents a system of n equations where all the elements of matrix $\mathbf{A}$ and vector $\mathbf{b}$ are known, and the equations are linear in the unknown elements of vector $\mathbf{x}$. If $\det(\mathbf{A}) \neq 0$ then the system has a unique solution for $\mathbf{x} = [x_1, x_2, \cdots, x_n]^T$ given by [30]

$$x_1 = \frac{\det(\mathbf{A}_1)}{\det(\mathbf{A})}, \quad x_2 = \frac{\det(\mathbf{A}_2)}{\det(\mathbf{A})}, \quad \cdots, \quad x_n = \frac{\det(\mathbf{A}_\mathrm{n})}{\det(\mathbf{A})},$$

where $\det(\mathbf{A}_j)$ is the matrix obtained by replacing the entries in the j^{th} column of $\mathbf{A}$ by the elements in the vector $\mathbf{b} = [b_1, b_2, \cdots, b_n]^T$.

To apply Cramer's rule, we first simplify Equations (3.54) and (3.56) by collecting the terms that are scaled by $\cos\lambda$ and $\sin\lambda$, and those that are independent of the angles as

$$\left.\begin{aligned} P_1\cos\lambda + Q_1\sin\lambda &= R_1, \\ P_2\cos\lambda + Q_2\sin\lambda &= R_2, \end{aligned}\right\} \tag{3.57}$$

where

$$\begin{aligned} P_1 &= 2X_C f, \\ Q_1 &= 2Y_C f, \\ R_1 &= X_C^2 + Y_C^2 + f^2 - a^2. \end{aligned} \quad \left\| \quad \begin{aligned} P_2 &= 2e\left((X_C - d)\cos\gamma + Y_C\sin\gamma\right), \\ Q_2 &= 2e\left(Y_C\cos\gamma - (X_C - d)\sin\gamma\right), \\ R_2 &= (X_C - d)^2 + Y_C^2 + e^2 - b^2. \end{aligned} \right.$$

We can now arrange these equations in the desired form as

$$\begin{bmatrix} P_1 & Q_1 \\ P_2 & Q_2 \end{bmatrix} \begin{bmatrix} \cos\lambda \\ \sin\lambda \end{bmatrix} \;\; = \;\; \begin{bmatrix} R_1 \\ R_2 \end{bmatrix}. \tag{3.58}$$

Note that the term $(X_C - d)^2$ in the coefficient R_2 in Equations (3.57) is obtained from the three terms $X_C^2 - 2dX_C + d^2$ in Equation (3.56). Solving Equations (3.57) using Cramer's rule for $\cos\lambda$ and $\sin\lambda$ yields

$$\cos\lambda = \frac{\begin{vmatrix} R_1 & Q_1 \\ R_2 & Q_2 \end{vmatrix}}{\begin{vmatrix} P_1 & Q_1 \\ P_2 & Q_2 \end{vmatrix}} = \frac{R_1Q_2 - R_2Q_1}{P_1Q_2 - P_2Q_1}, \quad \text{and} \tag{3.59}$$

$$\sin\lambda = \frac{\begin{vmatrix} P_1 & R_1 \\ P_2 & R_2 \end{vmatrix}}{\begin{vmatrix} P_1 & Q_1 \\ P_2 & Q_2 \end{vmatrix}} = \frac{P_1R_2 - P_2R_1}{P_1Q_2 - P_2R_1}. \tag{3.60}$$

Finally we enforce the identity $\cos^2\lambda + \sin^2\lambda = 1$ to obtain

$$(R_1Q_2 - R_2Q_1)^2 + (P_1R_2 - P_2R_1)^2 = (P_1Q_2 - P_2Q_1)^2,$$

or

$$(R_1Q_2 - R_2Q_1)^2 + (P_1R_2 - P_2R_1)^2 - (P_1Q_2 - P_2Q_1)^2 = 0. \tag{3.61}$$

The P_i and Q_i coefficients in Equation (3.61) are linear in the coordinates of the coupler point X_C and Y_C, while the R_i are quadratic. The products P_iR_j and Q_iR_j are therefore of order three $(1+2)$, and the squares of the differences are of order six $(3*2)$. Hence, the point coupler curve of an arbitrary planar $4R$ mechanism represented by Equation (3.61) is of order six (a *sextic*) agreeing with the well known theory of planar mechanisms [18].

3.6.1 Coupler Curve Examples

The following three examples of coupler curves from different mechanisms are intended to illustrate that the nature of any particular coupler point in any particular $4R$ linkage is tremendously varied. The first coupler curve plotted in Figure 3.15 (a) is for the non Grashof double π-rocker with link lengths in generic units of length of $a = 9$, $b = 12$, $d = 6$ and c implied by the coupler edge lengths $e = 8$ and $f = 8$, and the angle $\gamma = \frac{\pi}{3}$ between sides f and e, giving $c = \sqrt{e^2 + f^2 - 2ef\cos\gamma} = 8$, obviously, since the coupler triangle must be equilateral. Evaluating the signs of the three linear factors A_1, C_1, and D_1 from Equation (3.16) then consulting Table 3.1 reveals the linkage is indeed a non Grashof double π-rocker. Note the coupler curve possesses a single real crunode (real double point).

The second linkage is a non Grashof 0-rocker, π-rocker determined by $a = 6$, $b = 7$, $d = 12$ and c implied by the coupler edge lengths $e = 10$ and $f = 5$, and

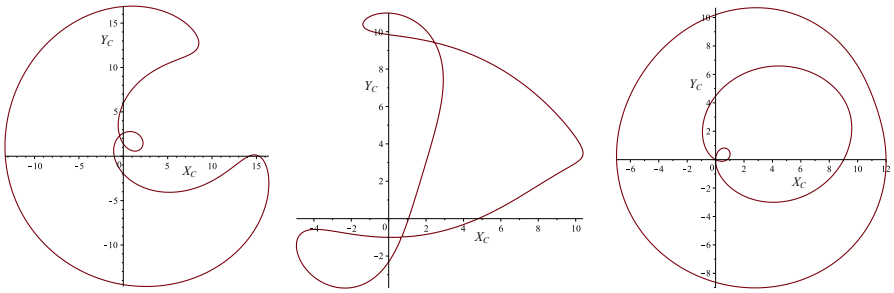

(a) (b) (c)

Figure 3.15: Three different coupler curves.

the angle $\gamma = \frac{\pi}{3}$ between sides f and e, giving $c = \sqrt{e^2 + f^2 - 2ef\cos\gamma} \approx 8.66$. The corresponding coupler curve is plotted in Figure 3.15 (b). This coupler curve possesses two real crunodes.

The third linkage is a Grashof double crank determined by $a = 6$, $b = 7$, $d = 4$ and c implied by the coupler edge lengths $e = 4$ and $f = 6$, and the angle $\gamma = \frac{\pi}{3}$ between sides f and e, giving $c = \sqrt{e^2 + f^2 - 2ef\cos\gamma} \approx 5.29$. The coupler curve, plotted in Figure 3.15 (c), has two distinct branches, one with a real crunode the other without. This illustrates a synthesis issue known as the *branch defect* because the linkage must be re-assembled in two different ways to reach both branches of the coupler curve.

3.6.2 Algebraic Properties of the Planar Coupler Curve

Discussion of the algebraic properties of the sextic coupler curve requires some knowledge of *plane algebraic curves* and *rational algebraic functions*. This material is discussed in great detail in [19], while the material presented in [20] is, in the author's own words: "intended to give the student a reasonably brief introduction to the subject". Some elementary material will be presented next to highlight the properties of these sextic curves. In particular, it is instructive to consider the *order* of the point equation of a curve as well as it's *circularity*, the *class* of the corresponding line equation of the curve, the number and type of *singular points*, and the *Plücker numbers* that relate them by virtue of the principle of duality. We will consider plane algebraic curves in general and the sextic coupler curve in particular in the following four subsections.

3.6.2.1 Curve Order; Bézout's Theorem; Imaginary Conjugate Circular Points; Circularity

A planar curve is *algebraic* if a point (x_1, x_2) which traces the curve satisfies an equation $f(x_1, x_2) = 0$, where f is a rational integral algebraic function of the coordinates x_1 and x_2. In other words a function is algebraic if

$$f(x_1, x_2) = \sum a_{ij} x_1^i x_2^j = 0$$

and the indices i and j take either finite integer values, or are zero, and a_{ij} is some constant rational coefficient (i.e. a ratio of two integers) for each unique term $x_1^i x_2^j$. The *degree* n of an algebraic planar curve is the highest power of x_1^i and x_2^j combined: $n = (i + j)_{\max}$. Clearly, the degree of a curve is a positive integer. In the study of algebraic curves, the degree of a particular curve is usually called it's *order*. When one, or more of the terms cannot be expressed as a rational number (a ratio of integers) it is said to be *irrational*. For example $x = e^y$, or $y = \cos x$ are *transcendental*, since the expressions for exponential and trigonometric functions represent infinite power series which cannot be represented as ratios of integers.

In 1876 Alfred Bray Kempe, a mathematician best known for his work on linkages, proved a theorem relating the properties of plane algebraic curves to planar linkages, which can contain only P- and R-pairs: it is theoretically possible to design a linkage to guide a point to trace any plane algebraic curve [31]. Regardless, since that time no general method has been discovered for identifying the best, or simplest mechanical system for tracing any particular plane algebraic curve [18]. Hence, there remains keen interest throughout the world for advancing and developing new knowledge in linkage design methods, performance metrics, and optimisation strategies. An excellent comprehensive introduction to plane algebraic curves may be found in [20] but is beyond the scope of this text. Nonetheless some of the concepts germane to planar four-bar analysis and design will now be introduced.

An arbitrary line in the plane cuts an n^{th} order algebraic curve in *at most* n points. A plane algebraic curve can be described by an equation as a locus of points, but it can also be described in a dual way by an equation as an envelope of lines tangent to the curve. In this case, a general point in the plane has *at most* n lines passing through it that are tangent to an algebraic curve of n^{th} class. Hence the distinction between the point equation and the line equation of a curve. Line equations will be discussed in greater detail later and are mentioned now only to hint at the great depth of the study of plane algebraic curves since antiquity. We will focus on point equations for the

moment. Generalising the notion of how many times a line cuts a n^{th} order algebraic curve we can eliminate the phrase "at most" from the theorem if we admit the existence of points of intersection that are imaginary, or infinite.

Because the point equation of a line is linear, it follows that it can intersect an n^{th} order algebraic curve in n points. By extension, Bézout's theorem states that two coplanar algebraic curves of orders n and m which do not share a common component, that is, which do not have infinitely many common points, intersect in general in nm points: the product of their orders. The theorem is named after Étienne Bézout who published a proof in 1779 in a treatise entitled *Théorie Générale des Équations Algébriques* [32], but the theorem was originally essentially stated without proof by Issac Newton in his proof of Lemma 28 in Volume 1 of his Principia in 1687 [33]. Regardless, history has justly recognised Bézout and the theorem bears his name.

It is easy to confirm by inspection that a line can cut a conic section in no more that two real points. Considering the plots in Figure 3.16, it is equally easy to confirm that two general coplanar conics, second order plane algebraic curves, can have at most four real points in common, unless they are coincident. If a right circular cone is cut by a plane parallel to it's base circle, but not at it's apex, the trace of the cone on the plane is a circle, a conic section, a general plane algebraic curve of order two. In fact, a circle is a special case of an ellipse whose major and minor axes have the same length. Yet two distinct coplanar circles never intersect in more than two real points. A circle cuts any other conic section in as many as four points, but not another circle! How is this so? Does this suggest that our Cartesian representation of the algebraic equation of a circle in the Euclidean plane E_2 is lacking the resolution needed to identify two additional points of intersection? Are there two additional points that are occluded by the representation using Cartesian coordinates? Let's examine the possibilities.

Consider the equation of an arbitrary circle, k, in the Euclidean plane E_2 with radius r and centre $\mathcal{C}(x_c, y_c)$:

$$(x - x_c)^2 + (y - y_c)^2 \quad = \quad r^2. \tag{3.62}$$

Expressing Equation (3.62) using homogeneous coordinates $x = \frac{x_1}{x_0},\ y = \frac{x_2}{x_0}$ produces the corresponding circle in the projective extension of E_2, called P_2:

$$\left(\frac{x_1}{x_0} - x_c\right)^2 + \left(\frac{x_2}{x_0} - y_c\right)^2 \quad = \quad r^2. \tag{3.63}$$

The homogenising coordinate x_0 can be considered a third length coordinate that has the effect of scaling the circle. In the case of a circle the value of x_0

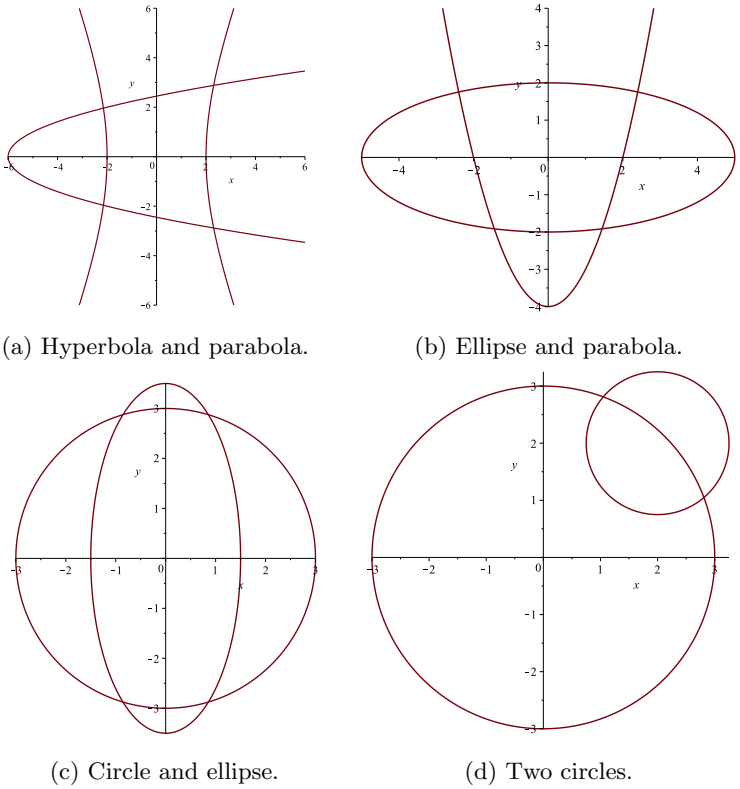

(a) Hyperbola and parabola.

(b) Ellipse and parabola.

(c) Circle and ellipse.

(d) Two circles.

Figure 3.16: Conic section intersections.

must be a positive number, or zero. When $x_0 = 1$ Equations (3.62) and (3.63) are identical. When the relative magnitude of x_0 increases, the circle becomes smaller and approaches it's centre. As $x_0 \Rightarrow \infty$ the circle diminishes in area until it becomes vanishingly small and ultimately degenerates to a single point: the centre. As x_0 diminishes, the area of the circle increases, with the limiting case being $x_0 = 0$. Equation (3.63) is now said to be *homogeneous* in x_0, x_1, and x_2. This is seen more readily if we multiply it by x_0^2 giving

$$(x_1 - x_c x_0)^2 + (x_2 - y_c x_0)^2 \quad = \quad r^2 x_0^2. \tag{3.64}$$

Now, every term in Equation (3.64) is homogeneously of degree two. When $x_0 = 1$ then $x_1 = 0$ and $x_2 = 0$ are the coordinate axes, but what happens when $x_0 = 0$ while x_1, x_2, x_c, y_c, and r remain finite? Just as lines $x_1 = 0$ and $x_2 = 0$ always intersect the circle in two real, or imaginary points, it must also be that the line $x_0 = 0$ intersects the circle in two points. Since the effect of setting $x_0 = 0$ gives the circle an infinitely large area and because $x_0 = 0$ is a line, it

must be that $x_0 = 0$ is a line at infinity. Because we are considering a circle in a plane, there can only be one line at infinity that bounds the finite locations in the plane. Hence, $x_0 = 0$ is called *the line at infinity*.

The intersection of a circle with the line at infinity $x_0 = 0$ is given by the equations

$$x_0 = 0, \quad x_1^2 + x_2^2 = 0. \tag{3.65}$$

In this case Equation (3.64) becomes

$$x_1^2 + x_2^2 \quad = \quad 0. \tag{3.66}$$

Equation (3.66) factors into a degenerate conic section consisting of a pair of complex conjugate imaginary lines

$$(x_1 + ix_2)(x_1 - ix_2) \quad = \quad 0 \tag{3.67}$$

which possess one real point of intersection, namely $(x_1, x_2) = (0, 0)$. Therefore, the line at infinity intersects the circle where the complex conjugate lines represented by Equation (3.67) meet the line at infinity, namely at the complex conjugate points I_1 and I_2:

$$(x_0 : x_1 : x_2) \quad = \quad \begin{cases} I_1(0 : i : 1), \\ I_2(0 : -i : 1). \end{cases} \tag{3.68}$$

The constants r, x_c and y_c which characterise the circle do not appear in the result. Thus, every circle represented in the projective extension of the Euclidean plane intersects the line at infinity in exactly the same two imaginary points, called the *conjugate imaginary circular points* I_1 and I_2. They are also widely called the *imaginary absolute circle points* [3, 16, 18, 22, 34]. It can be shown, in the same way, that every sphere cuts the plane at infinity in the imaginary conic:

$$x_0 = 0, \quad x_1^2 + x_2^2 + x_3^2 = 0, \tag{3.69}$$

which is called the *imaginary*, or *absolute sphere circle*.

These absolute quantities account for the apparent deficiency of Bézout's theorem [18, 35] for the intersections of algebraic curves and surfaces. That is, two curves of order n and m will intersect in nm points; similarly, two surfaces of order n and m will intersect in a curve of order nm. Clearly, two circles can intersect in at most two real points, while two spheres intersect in a circle (a second order curve). Since every circle contains the complex conjugate points I_1

and I_2, two circles can intersect in at most two more real points for a maximum number of four. The same applies for spheres; they intersect in a curve that, if it contains a real circle, always splits into a real and an imaginary conic. Hence Bézout's theorem is seen to be always true.

A *double point*, also known as a *node*, of a plane algebraic curve is a location where the curve intersects itself such that two branches of the curve have distinct tangent lines at that point. Double points are one type of singular point which will be elaborated on in greater detail in Subsection 3.6.2.4. Ordinary double points of plane curves are commonly known as *crunodes*. Ordinary double points of a plane curve given by $f(x_1, x_2) = 0$ must satisfy

$$f(x_1, x_2) = \frac{\partial f}{\partial x_1} = \frac{\partial f}{\partial x_2} = 0.$$

A non-degenerate planar algebraic curve of order n can have at most

$$\frac{1}{2}(n-1)(n-2) \tag{3.70}$$

double points, real and/or imaginary. Hence, a sextic coupler curve can have as many as

$$\frac{1}{2}(6-1)(6-2) = 10 \tag{3.71}$$

double points.

What does all this have to do with coupler curves? Because a circle contains the complex points I_1 and I_2 as two single complex conjugate points, a circle is said to have a *circularity* of one. Curves that contain I_1 and I_2 as double and triple points have circularity two and three, respectively. The circularity of the planar $4R$ coupler curve is determined by expressing the coordinates of the coupler point C as homogeneous coordinates $\frac{X_C}{W_C}$ and $\frac{Y_C}{W_C}$ in the point coupler curve equation, Equation (3.61). The only terms that remain after setting $W_C = 0$ represent the intersection of the general $4R$ coupler curve with the line at infinity:

$$\begin{aligned} &4\left((e\cos\gamma)^2 + (e\sin\gamma)^2 - 2ef\cos\gamma + f^2\right)(X_C^6 + Y_C^6) + \\ &\quad 12\left((e\cos\gamma)^2 + (e\sin\gamma)^2 - 2ef\cos\gamma + f^2\right)(X_C^4 Y_C^2 + X_C^2 Y_C^4) - \\ &\quad 16(e^2 f^2 \sin\gamma)^2 (X_C^4 + Y_C^4) - 32(ef\sin\gamma)^2 (X_C^2 + Y_C^2) = 0. \end{aligned}$$

It is to be understood that we are only considering non-degenerate point coupler curves, in which case the constant coefficients do not vanish. It is shown in [18] that the coupler curve intersects the line at infinity at points where

$$\left.\begin{aligned} W_C &= 0, \\ (X_C^2 + Y_C^2)^3 &= 0, \end{aligned}\right\} \tag{3.72}$$

namely at the complex conjugate circular points I_1 and I_2. We see that a planar $4R$ non-degenerate coupler curve has the imaginary circular points as triple points. Therefore the coupler curve has a circularity of three and is called a *tricircular sextic*. Since these are complex conjugate points, a $4R$ coupler curve can have at most four additional finite double points because Equation (3.70) indicates that a sextic curve has at most 10 double points, and six are always complex conjugates.

3.6.2.2 Duality

In the Euclidean plane a general line has the equation

$$Ax + By + C = 0 \tag{3.73}$$

where A, B, and C are arbitrary constants defining the slope and intercepts with the coordinate axes. The x and y that satisfy the equation are points on the line. Using homogeneous coordinates this linear equation becomes

$$X_0x_0 + X_1x_1 + X_2x_2 = 0 \tag{3.74}$$

where the X_i characterise lines (i.e., $X_0 = C$, $X_1 = A$, $X_2 = B$) and the x_i characterise points. Now Equation (3.74) represents Equation (3.73) as an equation that is linear in the X_i as well as the x_i. Every term in (3.74) is bilinear, or homogeneously linear. This should explain the etymology of the term homogeneous coordinates. The X_i are substituted for the A, B and C to underscore the bilinearity and symmetry. Now Equation (3.74) may be viewed as a range of variable points on a fixed line, or as a pencil of variable lines on a fixed point. The X_i define the line and are hence termed *line coordinates*, indicated by the ratios $[X_0 : X_1 : X_2]$; whereas the x_i define the point and bear the name *point coordinates*, indicated by the ratios $(x_0 : x_1 : x_2)$. Note that $[\cdots]$ are used to delimit line coordinates, while $(\cdots)$ are used to delimit point coordinates. Equation (3.74) is a bilinear equation describing the mutual incidence of point and line in the plane. Thus, point and line are considered as dual elements in the projective plane P_2. The importance of this concept is that any valid theorem concerning points and lines yields another valid theorem by simply exchanging these two words. For example, the proposition

> *any two distinct points determine one and only one line*

is dualised by exchanging the words point and line giving a very different proposition,

any two distinct lines determine one and only one point.

This topic is covered more thoroughly in *Chapter 5: Geometry* in this collection of notes and is introduced here as well for clarity in the description of the important duality between curve order and the next topic: class.

3.6.2.3 Class of a Line Equation

Given an arbitrary point in the plane and a plane algebraic curve that does not contain the point, the *class* of the curve is the number of lines that contain the point and are tangent to the curve. The class of a line equation of a curve is the line dual to the order of the point equation of the same curve. If the class is equal to m, then there are m lines tangent to the curve through the point, again these tangent lines may be real, imaginary, or at infinity. For curves of orders one and two the class is also one and two, respectively. For curves of order greater than two the class is generally a different positive integer. As a concept class is quite important because sometimes in kinematics a curve may be more efficiently expressed as the envelope of it's tangent lines rather than as the locus of it's points. This can be especially true when P- and R-pairs are both in the kinematic chain.

As an example consider the $PRRP$ linkage illustrated in Figure 3.17. Recall that this linkage is known as an elliptical trammel. When the P-pair longitudinal axes of symmetry are orthogonal the coupler, line AB, envelops a four pointed asteroid. The same asteroid would be traced by a circle of diameter $\frac{AB}{2}$ rolling without slip on the interior of the larger circle defined by the four singular apexes. Line AB has the homogeneous equation

$$\frac{x_1}{a\cos\vartheta} + \frac{x_2}{a\sin\vartheta} - x_0 \quad = \quad 0, \tag{3.75}$$

where a is the length of the coupler AB.

Again, an arbitrary line in the plane has the homogeneous equation

$$X_0x_0 + X_1x_1 + X_2x_2 \quad = \quad 0. \tag{3.76}$$

Comparing and equating the coefficients of x_1 and x_2 in Equations (3.75) and (3.76) yields

$$\left.\begin{array}{rcl} \dfrac{X_1}{X_0} & = & -\dfrac{1}{a\cos\vartheta}, \\ \dfrac{X_2}{X_0} & = & -\dfrac{1}{a\sin\vartheta}. \end{array}\right\} \tag{3.77}$$

The angle ϑ can be eliminated from the coefficients in Equation(3.75) with the line coefficients defined as in Equation(3.77) by squaring them and imposing

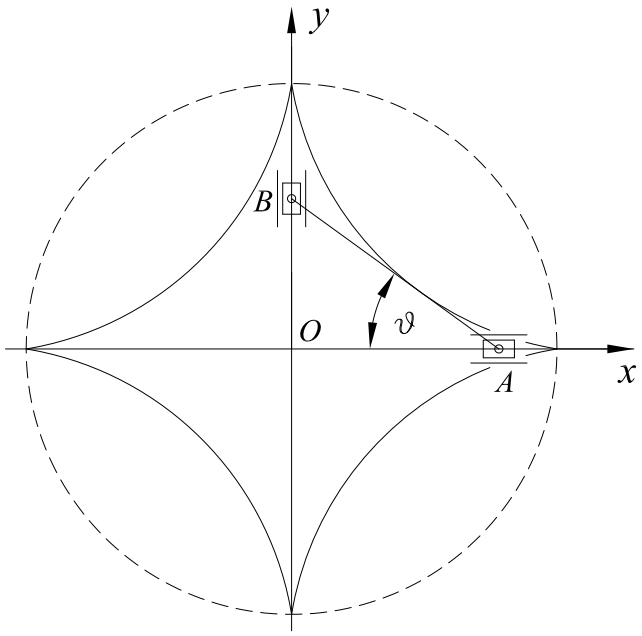

Figure 3.17: An asteroid is generated when the P-pairs in an $PRRP$ linkage are orthogonal.

the identity $\cos^2\vartheta + \sin^2\vartheta = 1$ which yields the line equation of the asteroid:

$$a^2X_1^2X_2^2 - X_0^2(X_1^2 + X_2^2) \quad = 0. \tag{3.78}$$

The line equation for the asteroid in Equation(3.78) is of degree four, therefore the class of the asteroid is $m = 4$. The locus of a point on a circle rolling without slip on a plane is known as a *cycloid*. Hence, because the point equation for the four pointed asteroid can be generated by a the locus of a point on the circle rolling without slip inside a circle of larger diameter it is also known as a *hypocycloid*.

Consulting the literature, one finds the point equation for the hypocycloid, or four pointed asteroid is

$$\left(a^2x_0^2 - (x_1^2 + x_2^2)\right)^3 - 27a^2x_0^2x_1^2x_2^2 \quad = \quad 0. \tag{3.79}$$

The point equation for the four pointed asteroid has order six, whereas the line equation for the very same curve is of class four.

3.6.2.4 Singular Points

In the study of kinematic geometry, and algebraic geometry in general, a *singular* point of a curve is a point P that is uniquely defined, hence singular. In the geometric sense, at this point the tangent space of the curve may not be regularly defined. A point that is not singular is a *regular*, or *simple point*. As we have seen in Subsection 3.6.2.1 a curve of order, or class, greater than two can intersect itself. The points where this happens are called *multiple points*. A comprehensive account of multiple points is to be found in [19]. The type of multiple point that occurs for planar $4R$ coupler curves are called *double points*, or *nodes*. The curve intersects itself a single time at a double point, hence there must be two tangents to the curve at that location. There are three species of double points that arise when the tangents to the curve at the double point are either a pair of distinct real lines, a pair of complex conjugate lines, or a pair of real but coincident lines.

To illustrate the different nature of the three types of double point consider the following cubic equation

$$y^2 \quad = \quad (x-a)(x-b)(x-c) \tag{3.80}$$

where the constant coefficients have rational positive magnitudes such that $a < b < c$. This curve, illustrated in Figure 3.18 (a), is symmetric with respect to the x-axis since every value of x gives equal and opposite values of y. The curve intersects the x-axis at the three points $x = a$, $x = b$, and $x = c$. When $x < a$ the value of y^2 is negative, and y is imaginary. When $a < x < b$ then y^2 is positive, and there are two real, equal and opposite values for y. For values of $b < x < c$ the value for y^2 is again negative, and finally positive again for all values $c < x$. The curve therefore consists of a closed oval between a and b and an open branch beginning at c and extending infinitely in two directions beyond it. The curve illustrated in Figure 3.18 has $a = 2$, $b = 4$, and $c = 5$. These values are then manipulated to yield a crunode, an acnode, and finally a cusp (spinode).

3.6.2.4.1 Crunode Now let b vary in magnitude between the range $a \leq b \leq c$. As b increases in value the oval circuit increases in size maintaining it's location at a but growing towards c until $b = c$ and the curve crosses itself. Inspecting the curve illustrated in Figure 3.18 (b) we see that at the double point, or node, the two branches of the curve meet, and each branch has it's own real, distinct tangent. Such a point is called a *crunode*.

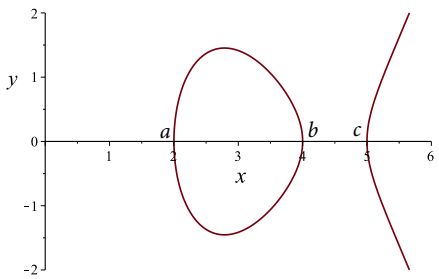

(a) Cubic with two real branches.

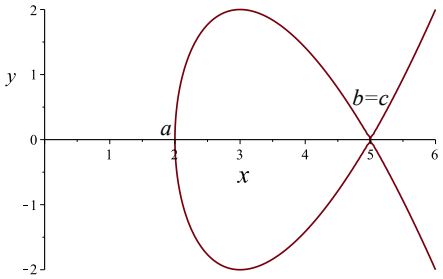

(b) A crunode.

Figure 3.18: Species of double points: crunode.

3.6.2.4.2 Acnode As b moves in the opposite direction towards a, the original oval circuit in Figure 3.18 (a) now shrinks in size until $b = a$. The cubic now possesses an isolated double point at $x = a = b$. Isolated points, also known as *hermit* points satisfy the equation of the cubic but do not appear to lie on the curve, see Figure 3.19 (a). Such points are called *acnodes*. The tangents to the curve at an acnode are complex conjugate lines. No real line through the acnode intersects the curve in more than one real point, confirming the necessary condition that a real line cuts a cubic in at most three points.

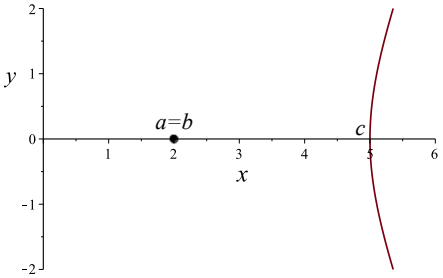

(a) An acnode.

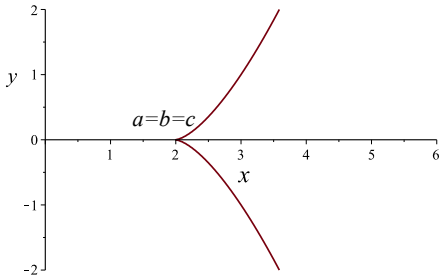

(b) A cusp, or spinode.

Figure 3.19: Species of double points: acnode and cusp (spinode).

3.6.2.4.3 Cusp (Spinode) The third species of double point occurs if the equation of the tangent to the curve at a point becomes a perfect square. In this case the tangents at the double point are two real, but coincident lines. In the case of the cubic in Equation (3.80) if we allow both coefficients b and c to approach a, the two distinct branches of the curve merge into a single branch

when $a = b = c$ and Equation (3.80) becomes

$$y^2 \quad = (x - a)^3. \tag{3.81}$$

This situation is illustrated in Figure 3.19 (b). The double point where $x = a = b = c$ is called a *cusp*, or a *spinode*. They are also sometimes called *stationary points* because if the curve is generated by the motion of a point then at a cusp the motion of the point in one direction comes to a stop and changes direction. The tangent at the cusp meets the curve in three coincident points at $(a, 0)$ in Figure 3.19 (b). An example we touched on earlier is the four pointed asteroid in Figure 3.17. It contains four real cusps at the coordinates $(\pm a, 0)$ and $(0, \pm a)$.

3.6.2.5 Plücker's Equations

When curves are generated as envelopes of tangent lines using line coordinates there are three dual characteristic numbers for the order of a curve point equation, it's number of cusps, and number of double points that are crunodes and acnodes. These dual quantities are the *class* of the curve line equation (as we have already discussed in Section 3.6.2.3), the number of *inflection points*, and the number of *bitangent lines*, respectively. The symbols corresponding to these quantities and the corresponding dual quantities pairs:

$$\left.\begin{array}{rcl} \text{order} & = & n \\ \text{class} & = & m \end{array}\right\} \quad \text{dual;}$$

$$\left.\begin{array}{rcl} \text{number of double points} & = & \delta \\ \text{number of bitangent lines} & = & \tau \end{array}\right\} \quad \text{dual;}$$

$$\left.\begin{array}{rcl} \text{number of cusps} & = & \kappa \\ \text{number of inflection points} & = & \iota \end{array}\right\} \quad \text{dual.}$$

The dual of a *cusp* is an *inflection point*. A cusp is generated when a point tracing the curve reaches a limit on it's path and changes direction while an inflection point is generated when a line enveloping a curve reaches a limiting gradient and then reverses. The dual of a *crunode* double point is a single line that is tangent to the curve at two distinct points and is called a *double tangent*, or *bitangent line*. The bitangent line, by analogy to an acnode, may have imaginary conjugate tangent points. In 1839 Julius Plücker published a comprehensive theory of algebraic curves [36] in which he identified five equations relating these six numbers. The versions presented here were derived in detail

in [20], while different useful versions are derived in [19]:

$$\left.\begin{array}{rcll} n(n-1) & = & m+2\delta+3\kappa; & \text{(a)} \\ m(m-1) & = & n+2\tau+3\iota; & \text{(b)} \\ 3n(n-2) & = & \iota+6\delta+8\kappa; & \text{(c)} \\ 3m(m-2) & = & \kappa+6\tau+8\iota; & \text{(d)} \\ 3(n-m) & = & \kappa-\iota. & \text{(e)} \end{array}\right\} \tag{3.82}$$

In this set of equations, enumerated simply as Equation (3.82), (a) and (b) are duals of each other, as are (c) and (d), while (e) is self-dual [18]. They may be cautiously used to establish limits on some of these numbers given knowledge of others, but they do not always unequivocally give answers. For example, one may compute the class of a curve if the order, number of double points, and number of cusps is known, but doubt may remain because of the need to distinguish between real and imaginary quantities as well as those at infinity.

3.7 Open Kinematic Chains

Recall from *Chapter 1: Introduction* that a kinematic chain is simple if each link in the chain is coupled to at most two other links. The degree of connectivity (DOC) of a link indicates the number of rigid bodies joined to it. If all links are binary ($DOC = 2$) the simple chain is closed. E.g. a four-bar mechanism. Alternately the simple chain is open with the first and last links having $DOC = 1$. Our analysis of planar four-bar mechanisms considered only closed simple kinematic chains, we now turn our attention briefly to the analysis of open chains.

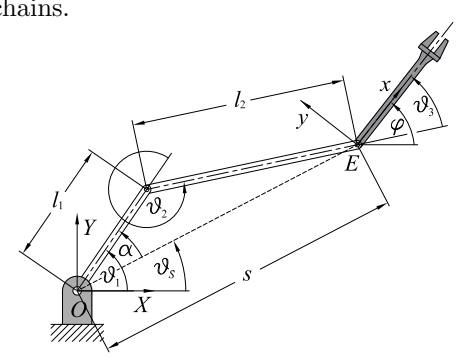

Figure 3.18. A $3R$ planar serial robotic arm.

Over the decades the study of the kinematics and kinetics of open kinematic chains has become largely associated with the study of the dynamics and control of industrial serial robots, see [37] for a comprehensive introduction. Since the focus of these notes is largely on closed kinematic chains the introduction given here is intended only to illustrate the difference between the analysis of closed and open chains. Consider the $3R$ planar serial robotic arm illustrated

in Figure 3.18. The two fundamental questions involved in the kinematic analysis of serially jointed robot arms are known as the *forward* and the *inverse* kinematics problems.

3.7.1 Forward Kinematics Problem

The forward kinematics problem involves computing the position and orientation of the end-effector given the individual joint angles. For the planar serial robot in Figure 3.18 this requires determining the location of the origin of the end-effector reference coordinate system, point E in this case, and the angle the x-axis makes with respect to the X-axis of the non-moving ground-fixed reference coordinate system with origin located at point O, given the joint angles, in this case ϑ_1, ϑ_2, and ϑ_3.

Because this is a planar problem, the absolute orientation of the end-effector reference coordinate system with respect to the X-axis, let's call it φ, is simply the sum of the three relative joint angles:

$$\varphi \quad = \quad \vartheta_1 + \vartheta_2 + \vartheta_3. \tag{3.83}$$

To compute the location of the origin E of the end-effector coordinate system the usual approach is to concatenate the appropriate homogeneous transformation matrices. However, in the planar case we may simply use the law of cosines. Because ϑ_2 is the external angle of edge l_2 with respect to edge l_1 of triangle $\triangle l_1 l_2 s$ we can use the alternate form of the cosine law to compute the distance s between origins O and E as

$$s \quad = \quad \sqrt{l_1^2 + l_2^2 + 2 l_1 l_2 \cos \vartheta_2}. \tag{3.84}$$

The angle that line s makes with respect to the X-axis is ϑ_s, given by

$$\vartheta_s \quad = \quad \vartheta_1 - \alpha \quad = \quad \vartheta_1 - \cos^{-1}\left(\frac{l_1^2 s^2 - l_2^2}{2 l_1 s}\right). \tag{3.85}$$

Finally, the position vector of E in the ground fixed coordinate system with origin at O is

$$\mathbf{E} \quad = \quad \begin{bmatrix} s\cos\vartheta_s \\ s\sin\vartheta_s \end{bmatrix}. \tag{3.86}$$

3.7.2 Inverse Kinematics Problem

The inverse kinematics problem involves computing the joint angles ϑ_1, ϑ_2, and ϑ_3 required to to give the moving coordinate system with origin E a particular

position and orientation within the reachable workspace of the arm. Since the position and orientation of the coordinate system that moves with E is given we know the angle φ and the position vector $\mathbf{E}$, and hence length s, using trigonometry and the cosine law we can compute

$$\vartheta_s = \tan^{-1}\left(\frac{E_Y}{E_X}\right), \quad \text{and} \quad \alpha = \cos^{-1}\left(\frac{l_1^2 + s^2 - l_2^2}{2l_1 s}\right). \tag{3.87}$$

Next we compute

$$\vartheta_1 = \vartheta_s + \alpha. \tag{3.88}$$

We again use the cosine law to obtain

$$\vartheta_2 \quad = \quad \cos^{-1}\left(\frac{l_1^2 + l_2^2 - s^2}{2l_1 l_2}\right). \tag{3.89}$$

Finally, since we are given the angle φ we can determine the last joint angle with Equation (3.83)

$$\vartheta_3 \quad = \quad \varphi - \vartheta_1 - \vartheta_2. \tag{3.90}$$

Of course, there are usually more than one solution, and in order for a solution to exist it must be that the goal point given by length s is located within the reachable workspace of the arm such that $s \leq l_1 + l_2$.

Bibliography

[1] Euclid. *The Thirteen Books of the Elements,* second edition, translation by Sir T. L. Heath, vol's 1,2,3. Dover Publications, Inc., New York, N.Y., U.S.A., 1956.

[2] T.Q. Sibley. *Thinking Geometrically: A Survey of Geometries.* The Mathematical Association of America, Washington, DC, U.S.A., 2015.

[3] F. Klein. *Elementary Mathematics from an Advanced Standpoint: Geometry.* Dover Publications, Inc., New York, N.Y., U.S.A., 1939.

[4] J. Angeles. *Spatial Kinematic Chains: Analysis, Synthesis, Optimization.* Springer-Verlag, New York, N.Y., U.S.A., 1982.

[5] M.J.D. Hayes, M.L. Husty, and M. Pfurner. "Input-output Equation for Planar Four-bar Linkages". *Advances in Robot Kinematics 2018,* eds. J. Lenarčič and V. Parenti-Castelli*, Springer, New York*, pages 12–19, 2018.

[6] M.L. Husty and M. Pfurner. "An Algebraic Version of the Input-output Equation of Planar Four-bar Mechanisms". *ICGG 2018 - Proceedings of the 18th International Conference on Geometry and Graphics,* ed. L. Cocchiarella*, Springer, New York*, pages 775–786, 2018.

[7] F. Freudenstein. "An Analytical Approach to the Design of Fourlink Mechanisms.". *Trans. ASME*, vol 77: pages 483–492, 1954.

[8] F. Freudenstein. "Approximate Synthesis of Four-Bar Linkages". *Trans. ASME 77,* pages 853-861, 1955.

[9] S. O. Tinubu and K. C. Gupta. "Optimal Synthesis of Function Generators Without the Branch Defect". *ASME, J. of Mech., Trans., and Autom. in Design*, vol. 106: pages 348354, 1984.

[10] M.J.D. Hayes, K. Parsa, and J. Angeles. "The Effect of Data-Set Cardinality on the Design and Structural Errors of Four-Bar Function-Generators". *Proceedings of the Tenth World Congress on the Theory of Machines and Mechanisms,* Oulu, Finland, pages 437–442, 1999.

[11] A. Guigue and M.J.D. Hayes. "Continuous Approximate Synthesis of Planar Function-generators Minimising the Design Error". *Mechanism and Machine Theory*, vol. 101: pages 158–167, DOI: 10.1016/j.mechmachtheory.2016.03.012, 2016.

[12] D. J. Wilde. "Error Synthesis in the Least-Squares Design of Function Generating Mechanisms". *ASME, J. of Mechhanical Design*, 104:881–884, 1982.

[13] G. Dahlquist and Å. Björck. *Numerical Methods,* translated from Swedish by N. Anderson. Prentice-Hall, Inc., U.S.A., 1969.

[14] F. Freudenstein. *Design of Four-link Mechanisms.* PhD thesis, Columbia University, New York, N.Y., USA, 1954.

[15] E. Study. *Geometrie der Dynamen.* Teubner Verlag, Leipzig, Germany, 1903.

[16] O. Bottema and B. Roth. *Theoretical Kinematics.* Dover Publications, Inc., New York, N.Y., U.S.A., 1990.

[17] M.J.D. Hayes and M.L. Husty. "On the Kinematic Constraint Surfaces of General Three-Legged Planar Robot Platforms". *Mechanism and Machine Theory*, vol. 38, no. 5: pages 379–394, 2003.

[18] K.H. Hunt. *Kinematic Geometry of Mechanisms.* Clarendon Press, Oxford, England, 1978.

[19] G. Salmon. *A Treatise on the Higher Plane Curves,* third edition. Hodges, Foster, and Figgis, Dublin, Rep. of Ireland, 1879.

[20] E.J.F. Primrose. *Plane Algebraic Curves.* Macmillan & Co. LTD., London, England, 1955.

[21] H.S.M. Coxeter. *Introduction to Geometry,* 2^{nd} edition. University of Toronto Press, Toronto, On., Canada, 1969.

[22] H.S.M. Coxeter. *Projective Geometry,* 2^{nd} edition. University of Toronto Press, Toronto, On., Canada, 1974.

[23] D. Gans. *Transformations and Geometries.* Appelton-Century-Crofts, New York, N.Y., U.S.A., 1969.

[24] A.P. Murray and P.M. Larochelle. "A Classification Scheme for Planar $4R$, Spherical $4R$, and Spatial $RCCR$ Linkages to Facilitate Computer Animation". Proceedings of 1998 ASME Design Engineering Technical Conferences (DETC'98)*, Atlanta, Georgia, U.S.A.*, September 13-16, 1998.

[25] J.M. McCarthy and G.S. Soh. *Geometric Design of Linkages, 2nd Edition* Interdiciplinaty Applied Mathematics. Springer, New York, N.Y., 2011.

[26] F. Grashof. *Theoretische Maschinenlehre,* vol. 2. Voss, Hamburg, Germany, 1883.

[27] M. Ceccerelli, editor. *Distinguished Figures in Mechanism and Machine Science, Their Contributions and Legacies Part 1.* Springer, New York, U.S.A., 2007.

[28] J.E. Shigley and J.J. Uicker, Jr. *Mechanism and Machine Theory, 2nd ed.* McGraw-Hill, New York, N.Y., U.S.A., 1995.

[29] S. Roberts. "On the Motion of a Plane Under Certain Conditions". *Proceedings of the London Mathematical Society*, vol. 4: pages 286–318, 1871.

[30] H. Anton. *Elementary Linear Algebra, 5th Ed.* Wiley, New York, N.Y., U.S.A., 1987.

[31] A.B. Kempe. "On a General Method of Describing Plane Curves of the n^{th} Degree by Linework". *Proceedings of the London Mathematical Society*, vol. 7: pages 213–216, 1876.

[32] E. Bézout. *Théorie Générale des Équations Algébriques.* Kessinger Publishing, Whitefish, MT., U.S.A., 1779.

[33] I. Newton. *The Principia: Mathematical Principles of Natural Philosophy,* English translation by I.B. Cohen, A. Whitman, J. Budenz. University of California Press (Feb. 5 2016), U.S.A., 1687.

[34] D.M.Y. Sommerville. *Analytical Geometry of Three Dimensions.* Cambridge University Press, London, England, 1934.

[35] G. Salmon. *Lessons Introductory to the Modern Higher Algebra,* 4^{th} edition. Hodges, Foster, and Figgis, Dublin, Rep. of Ireland, 1885.

[36] J. Plücker. *Theorie der algebraischen Curven.* Adolph Marcus, Bonn, Germany, 1839.

[37] J.J. Craig. *Introduction to Robotics, Mechanics and Control,* 4^{th} edition. Pearson, London, England, 2017.